High-spin structures of five $N = 82$ isotopes: $^{136}_{54}$Xe, $^{137}_{55}$Cs, $^{138}_{56}$Ba, $^{139}_{57}$La, and $^{140}_{58}$Ce

A. Astier,[1] M.-G. Porquet,[1] Ts. Venkova,[1,2] D. Verney,[3] Ch. Theisen,[4] G. Duchêne,[5] F. Azaiez,[5,*] G. Barreau,[6] D. Curien,[5] I. Deloncle,[1] O. Dorvaux,[5] B. J. P. Gall,[5] M. Houry,[4,†] R. Lucas,[4] N. Redon,[7] M. Rousseau,[5] and O. Stézowski[7]

[1]*CSNSM, IN2P3-CNRS and Université Paris-Sud, Bâtiment 104-108, F-91405 Orsay, France*

[2]*INRNE, BAS, 1784 Sofia, Bulgaria*

[3]*IPNO, IN2P3-CNRS and Université Paris-Sud, F-91406 Orsay, France*

[4]*CEA, Centre de Saclay, IRFU/Service de Physique Nucléaire, F-91191 Gif-sur-Yvette Cedex, France*

[5]*IPHC, IN2P3-CNRS and Université Louis Pasteur, F-67037 Strasbourg Cedex 2, France*

[6]*CENBG, IN2P3-CNRS and Université Bordeaux I, F-33175 Gradignan, France*

[7]*IPNL, IN2P3-CNRS and Université Claude Bernard, F-69622 Villeurbanne Cedex, France*

(Received 25 April 2012; revised manuscript received 23 May 2012; published 15 June 2012)

Five $N = 82$ isotones have been produced in two fusion-fission reactions and their γ rays studied with the Euroball array. The high-spin states of ^{139}La have been identified, while the high-spin yrast and near-to-yrast structures of the four others have been greatly extended. From angular correlation analysis, spin values have been assigned to some states of ^{136}Xe and ^{137}Cs. Several cascades involving γ rays of ^{139}La have been found to be delayed; they deexcite an isomeric state with $T_{1/2} = 315(35)$ ns located at 1800 keV excitation energy. The excited states of these five $N = 82$ isotones are expected to be due to various proton excitations involving the three high-j subshells located above the $Z = 50$ shell closure. This is confirmed by the results of shell-model calculations performed in this work. In addition, high-spin states corresponding to the excitation of the neutron core have been unambiguously identified in ^{136}Xe, ^{137}Cs, and ^{138}Ba.

DOI: 10.1103/PhysRevC.85.064316 PACS number(s): 23.20.Lv, 21.60.Cs, 25.70.Jj, 27.60.+j

I. INTRODUCTION

The study of the low-lying excited states of the $N = 82$ isotones offers the best ground to describe the gradual filling of the active proton orbitals lying above the $Z = 50$ closure, since these states are free of any neutron contribution up to an excitation energy of about 4 MeV. Particularly, the description of the high-spin states mainly involves the effective interactions of the protons when occupying the valence orbits, particularly the high-j ones, $\pi g_{7/2}$, $\pi d_{5/2}$, and $\pi h_{11/2}$, which can thus be tested. Many years ago, a lot of low-spin states of several $N = 82$ isotones were used to define the two-body part of the shell-model Hamiltonian [1], which was adjusted some time later [2] using new data on some high-spin states of the "light" $N = 82$ isotones produced by spontaneous fission of actinides [3,4]. This set of empirical interactions was then tested on the new high-spin states of ^{137}Cs, identified in a deep-inelastic reaction up to $I^{\pi} = (31/2^{-})$ [5].

By combining appropriate fusion-fission reactions with a powerful γ-detection array, it is possible to populate and to study the high-spin states of many $N = 82$ isotones. In this paper, we present our results obtained on the high-spin states of five isotones, $^{136}_{54}$Xe, $^{137}_{55}$Cs, $^{138}_{56}$Ba, $^{139}_{57}$La, and $^{140}_{58}$Ce, which have been identified in two Euroball experiments. The level schemes of four of them have been well extended to higher-spin values. The high-spin structures of ^{139}La have been identified, displaying an isomeric state with $T_{1/2} = 315(35)$ ns located at 1800 keV excitation energy. The states of these five $N = 82$ isotones are then compared to the results of shell-model calculations using the set of empirical interactions already used to describe the lightest isotones. In addition, groups of states lying above 4 MeV excitation energy in ^{136}Xe, ^{137}Cs, and ^{138}Ba are assigned to the excitation of the neutron core.

II. EXPERIMENTAL DETAILS

A. Reactions, γ-ray detection, and analysis

The $N = 82$ isotones of interest were obtained as fission fragments in two experiments. First, the ^{12}C + ^{238}U reaction was studied at 90 MeV incident energy, with a beam provided by the Legnaro XTU Tandem accelerator. Second, the ^{18}O + ^{208}Pb reaction was studied with a 85 MeV incident energy beam provided by the Vivitron accelerator of IReS (Strasbourg). The gamma rays were detected with the Euroball array [6]. The spectrometer contained 15 cluster germanium detectors placed in the backward hemisphere with respect to the beam, 26 clover germanium detectors located around 90°, and 30 tapered single-crystal germanium detectors located at forward angles. Each cluster detector consists of seven closely packed large-volume Ge crystals [7] and each clover detector consists of four smaller Ge crystals [8]. In order to get rid of the Doppler effect, both experiments have been performed with thick targets in order to stop the recoiling nuclei (47 mg/cm^2 for ^{238}U and 100 mg/cm^2 for ^{208}Pb targets, respectively).

The data of the (C + U) experiment were recorded in an event-by-event mode with the requirement that a minimum of five unsuppressed Ge detectors fired in prompt coincidence. A set of 1.9×10^9 three- and higher-fold events was available

[*]Present address: IPNO, IN2P3-CNRS and Université Paris-Sud, F-91406 Orsay, France.

[†]Present address: CEA/DSM/Département de recherches sur la Fusion Contrôlée, F-130108 Saint-Paul lez Durance, France.

for a subsequent analysis. For the (O + Pb) experiment, a lower trigger condition (three unsuppressed Ge) allowed us to register 4×10^9 events with a γ-fold greater than or equal to 3. The offline analysis consisted of both multigated spectra and three-dimensional "cubes" built and analyzed with the RADWARE package [9].

More than one hundred nuclei are produced at high spin in such experiments, and this gives several thousands of γ transitions which have to be sorted out. Single-gated spectra are useless in most of the cases. The selection of one particular nucleus needs at least two energy conditions, implying that at least two transitions have to be known. The identification of transitions depopulating high-spin levels which are completely unknown is based on the fact that prompt γ rays emitted by complementary fragments are detected in coincidence [10,11]. Moreover, because the isotopes of interest are produced from two different fissioning compound nuclei, the complementary fragments are different in the two reactions. This gives a fully unambiguous assignment of transitions seen in both experiments.

B. Isomer identification

As reported in previous papers [12,13], another experiment was performed using the SAPhIR[1] heavy-ion detector [14], here composed of 32 photovoltaic cells, in order to identify new isomeric states in the fission fragments. Placed in the target chamber of Euroball, SAPhIR was used to detect the escaping fission-fragments of the ^{12}C (90 MeV) + ^{238}U reaction from a thin 0.14 mg/cm^2 uranium target. Thus, all recorded γ rays emitted at rest by a fragment implanted in SAPhIR correspond to the decay of an isomeric state, for which the half-life can be measured in a range of several tens to several hundreds of nanoseconds.

C. $\gamma - \gamma$ angular correlations

It is well known that the γ rays emitted by fusion-fission fragments do not show any anisotropy in their angular distributions with respect to the incident beam. However, angular correlations of two successive transitions are meaningful. In order to determine the spin values of excited states, the coincidence rates of two successive γ rays are analyzed as a function of θ, the average relative angle between the two fired detectors. The Euroball spectrometer had $C^2_{239} = 28\,441$ combinations of two crystals, out of which only $\sim$2000 involved different values of relative angle within 2°. Therefore, in order to keep reasonable numbers of counts, all these angles have been gathered around three average relative angles: 22°, 46°, and 75°. The coincidence rate is increasing between 0° and 90° for the dipole-quadrupole cascades, whereas it decreases for the quadrupole-quadrupole or dipole-dipole ones. The theoretical values of several coincidence rates for the Euroball geometry have been already given in previous papers [15,16]. The method has been checked by correctly reproducing the expected angular correlations of γ transitions having well known multipole orders and belonging to various fission fragments.

[1]SAPhIR, Saclay Aquitaine Photovoltaic cells for Isomer Research.

III. EXPERIMENTAL RESULTS

A. Study of the odd-Z isotones

1. Level scheme of $^{137}_{55}Cs$

The yrast states of ^{137}Cs were obtained up to $\sim$5.5 MeV from the analysis of the ^{248}Cm spontaneous-fission study [5]. More recently a few transitions were added to this level scheme, using a ^{252}Cf source [17]. Nevertheless the spin-parity values were only based on results of shell-model calculations.

In our work, γ rays emitted by ^{137}Cs are seen in the two fusion-fission reactions, with a slightly higher production in the C + U reaction compared to the O + Pb one, especially for the high-spin states. The high-spin level scheme of ^{137}Cs has been extended up to $\sim$7.6 MeV excitation energy and spin $(37/2^+)$, thanks to the observation of about 25 new transitions (see Fig. 1).

A 681-keV transition, already identified in the two previous experiments, is also oberved in our work, being located just above the 2783-keV level (Structure B). The coincidence relationships of this γ line involve the four yrast transitions, but we could not observe any transition located above the 3464-keV level, although the intensity of the 681-keV transition would have allowed us to see a higher-spin part of the cascade. This level is likely populated by several high-energy transitions which have escaped from our detection apparatus.

We do not confirm two of the six new transitions above the 1893-keV level, which were proposed by the authors of Ref. [17] in addition to the previous level scheme [5]. The 2223.6- and 1609.4-keV γ rays are not observed in coincidence with the first yrast transitions. Moreover the decay of the 3495-keV level toward the 3302-keV one by means of a 193-keV transition is not observed.

The most noticeable information obtained in this work is the observation of two structures composed of low-energy transitions (therefore presumably $M1$) located above the 4350- and 5452-keV levels (Structures C and D in Fig. 1). The decays of their low-lying states are very fragmented and involve high-energy transitions. An example of double-gated spectrum showing the first transitions of Structure D and its links to Structure E is given in Fig. 2.

Angular correlations of successive γ rays have been extracted for the most intense transitions of ^{137}Cs. The experimental results are given in Table I. The three first results indicate that the transitions at 1184, 487, and 890 keV have the same multipole order, while the last one indicates that the multipole order of the 222-keV transition is different from that of the three others. An $E2$ character is ruled out for the 222-keV transition, because the 1893-keV level would then be an isomeric state, with a half-life of a few tens to a few hundreds of ns, at variance with the fact that the 1184-487-222 keV cascade is not observed in the SAPhIR experiment. Thus the 222-keV transition is assigned to be a dipole transition, while the 1184-, 487-, and 890-keV transitions have an $E2$ character. These arguments result in the spin values of $11/2^+$, $15/2^+$,

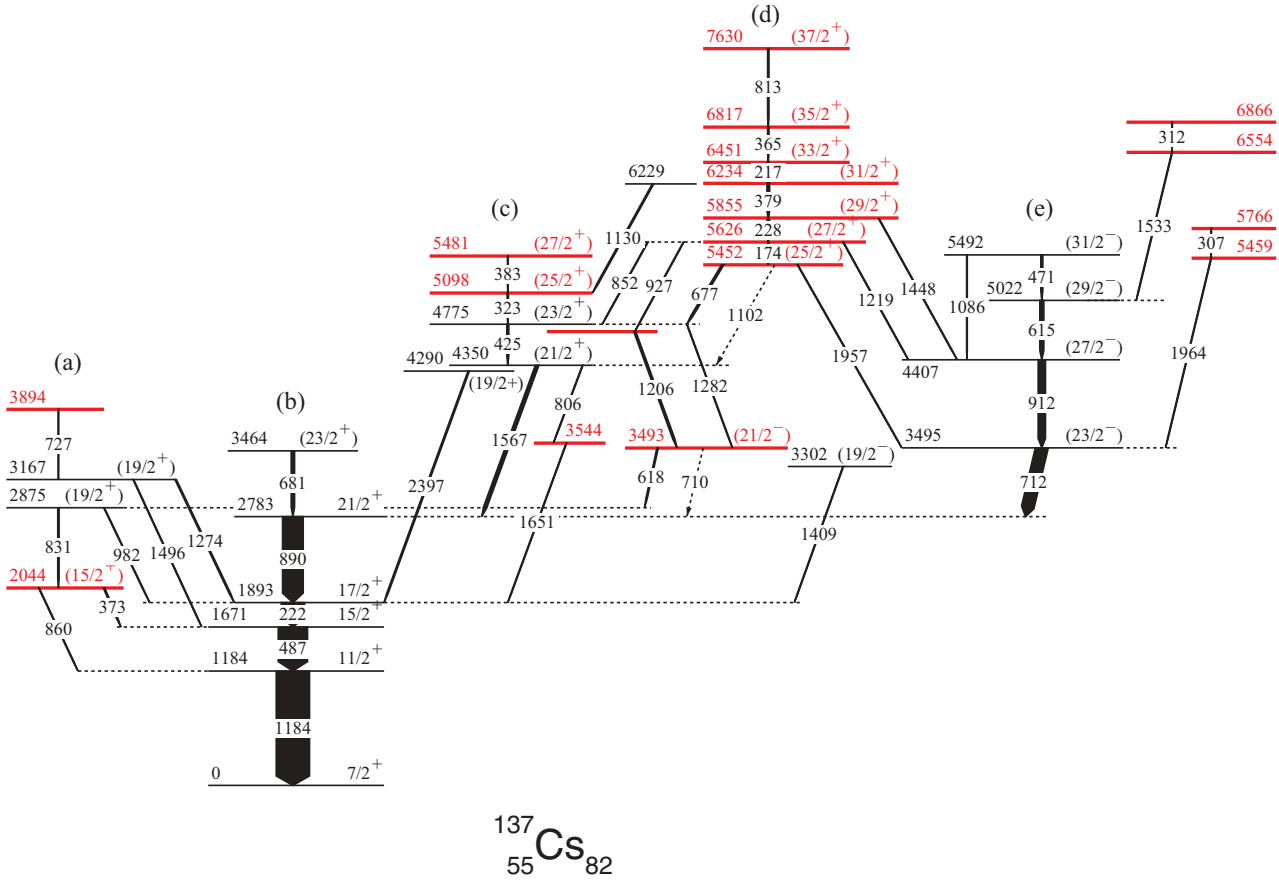

FIG. 1. (Color online) Level scheme of ^{137}Cs established in this work. The colored states are new. The width of the arrows is proportional to the γ-ray intensity.

$17/2^+$, and $21/2^+$ for the levels at 1184, 1671, 1893, and 2783 keV, belonging to Structure B.

The spin assignments of the higher-lying states are based on the following assumptions: (i) In the yrast decays, spin values increase with excitation energy, and (ii) the low-energy transitions have a $M1$ character. In addition, the negative parity proposed in Ref. [5] for the states of the group labeled E because of the comparison with calculations is in agreement with its single link to the $21/2^+$ state. The parity of the states of Structures C and D will be discussed in Sec. IV C2, from the comparison with theoretical predictions.

The properties of the ^{137}Cs transitions are given in Table II. The intensity values have been extracted as follows: First, the ratio $I_\gamma(487\text{keV})/I_\gamma(1184\text{keV}) = 0.88$ has been measured in a spectrum built with double gates set on its main complementary fragments (^{103,105}Tc) in the (C + U) experiment. Then, the spectrum gated simultaneously on the 1184-keV γ-ray and Tc transitions gives the 222-keV intensity relative to the 487-keV one. Finally, all other intensities have been measured from spectra built with double gates set on ^{137}Cs transitions.

2. *Level scheme of* $^{139}_{57}La$

High-spin states in ^{139}La were scarcely known before our work. Four states with $I = 9/2$ and two states with $I = 11/2$ have been proposed from the $(n, n'\gamma)$ reaction, at an excitation energy below 1.6 MeV [18], most of these states directly decaying to the ground state. Thus in order to identify the γ-ray cascades emitted by the high-spin states of ^{139}La, we have first used double-gated spectra on transitions of ^{101,102,103}Nb isotopes [19], the complementary fragments of ^{139}La in the (C + U) fusion-fission experiment. We cannot confirm the existence of a $9/2^+$ state at 1219 keV, which should have been the yrast one, since we do not observe any of the 1219- or 1051-keV transitions [18]. However we confirm the $(9/2^+)$ state at 1381 keV, thanks to its decay toward the $5/2^+$ level (located at 166 keV), *via* the 1215-keV line which is in clear coincidence with the known 166-keV $5/2^+ \rightarrow 7/2^+$ transition. The 1215-keV transition is one of the strongest transition observed in coincidence when gating directly on the complementary fragments. The two other reported $9/2^+$ levels, being non-*yrast*, cannot be identified in our experiment. Secondly, the 166–1215 two-gate spectrum easily reveals, in addition to Nb transitions, many new γ lines which have to be located above the 1381-keV state of ^{139}La. Finally, all the coincidence relationships between these new transitions have been carefully analyzed in order to build the level scheme shown in Fig. 3.

Two levels at very close excitation energies are reported in the literature at 1537.7 and 1537.9 keV, with proposed spin assignments of $(11/2^+)$ for the former, which only decays

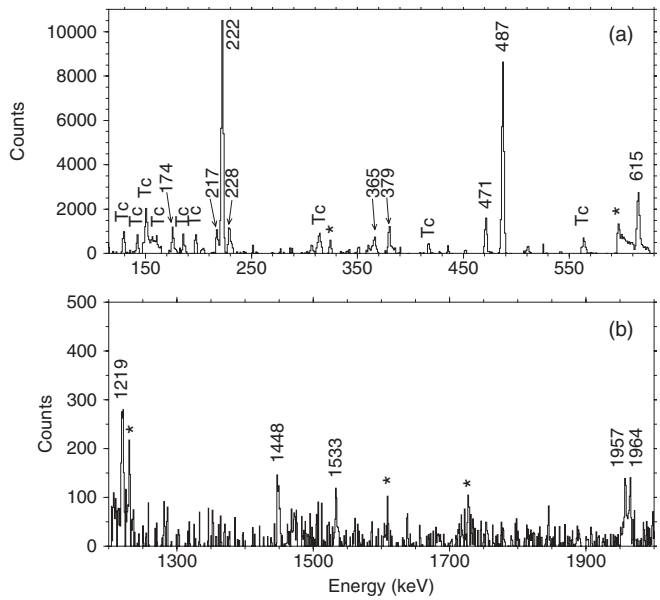

FIG. 2. Spectrum of γ rays in coincidence with two transitions of ^{137}Cs showing the first transitions of Structure D in the low-energy part (a) and the links between Structures D and E in the high-energy part (b). The first gate is set on the 712-keV transition and the second gate is set on one of the four yrast transitions (1184, 487, 222, and 890 keV). Transitions emitted by ^{103,104,105}Tc, the complementary fragments of ^{137}Cs, are labeled by Tc. The peaks marked with a star are contaminants.

to the ground state, and $7/2^+$ for the latter, which populates equally the ground state and the first excited state at 166 keV [18]. The 1537-keV γ line is only present in our data in coincidence with the Nb transitions, meaning that only the $(11/2^+)$ state has been populated in our experiment.

A second doublet of close-lying states is known at 1420.5 and 1420(12) keV [18]. The first one, populated in the β decay of ^{139}Ba ($I^\pi_{gs} = 7/2^-$) with $\log_{10} ft = 7.6$, shows a main decay to the ground state and a weak component to the first excited state (9%). The second one was populated with a $L = 5$ transfer in (^{3}He,d), (d,^{3}He), and (^{7}Li, ^{6}He) reactions [18], and was thus assigned as $I^\pi = 11/2^-$ (from the $\pi h_{11/2}$ orbit). Its γ decay, not measured, likely involves two branches, one toward the ground state with an $M2$ multipolarity and one toward the 166-keV level with an $E3$ multipolarity; i.e., similar to those measured in the neighboring isotones, ^{141}Pr and ^{143}Pm [18]. Thus such a deexcitation is the same as that measured for the 1420.5-keV level identified in the β decay of ^{139}Ba. This could indicate that there is only one state at 1420.5 keV. Nevertheless the measured value of the direct β feeding is too high for a second-forbidden nonunique transition ($\Delta J = 2$, $\Delta\pi = +$). Thus the results of β decay and transfer reactions cannot be

TABLE I. Coincidence rates between the low-lying γ rays of ^{137}Cs as a function of their relative angle of detection, normalized by the ones obtained around 75°.

γ-γ coincidence	$R(22°)$[a]	$R(46°)$[a]	$R(75°)$[a]
1184 - 487	1.19(9)	1.07(8)	1.00(6)
890 - 487	1.20(8)	1.08(7)	1.00(4)
890 - 1184	1.09(9)	1.07(7)	1.00(6)
222 - 1184	0.93(7)	0.99(6)	1.00(5)

[a]The number in parentheses is the error in the last digit.

TABLE II. Properties of the transitions assigned to ^{137}Cs observed in this work.

E_γ[a] (keV)	I_γ[a,b]	$I_i^\pi \rightarrow I_f^\pi$	E_i	E_f
174.4(3)	4.5(22)	$(27/2^+) \rightarrow (25/2^+)$	5626.5	5452.2
216.9(3)	5.5(20)	$(33/2^+) \rightarrow (31/2^+)$	6451.3	6234.4
221.8(3)	70(10)	$17/2^+ \rightarrow 15/2^+$	1893.0	1671.2
228.5(3)	8.2(25)	$(29/2^+) \rightarrow (27/2^+)$	5855.0	5626.5
306.7(4)	1.0(5)		5766.1	5459.4
311.9(4)	1.0(5)		6866.1	6554.2
323.5(4)	3.8(19)	$(25/2^+) \rightarrow (23/2^+)$	5098.2	4774.7
365.4(6)	4.0(20)	$(35/2^+) \rightarrow (33/2^+)$	6816.7	6451.3
372.6(4)	3.5(17)	$(15/2^+) \rightarrow 15/2^+$	2043.8	1671.2
379.4(4)	8.4(25)	$(31/2^+) \rightarrow (29/2^+)$	6234.4	5855.0
383.3(4)	3.5(17)	$(27/2^+) \rightarrow (25/2^+)$	5480.5	5098.2
424.9(4)	5.9(24)	$(23/2^+) \rightarrow (21/2^+)$	4774.7	4349.8
470.6(4)	4.5(18)	$(31/2^-) \rightarrow (29/2^-)$	5492.2	5021.6
486.8(3)	88(13)	$15/2^+ \rightarrow 11/2^+$	1671.2	1184.4
614.8(4)	11(3)	$(29/2^-) \rightarrow (27/2^-)$	5021.6	4406.8
618.0(4)	3.4(17)	$(21/2^-) \rightarrow (19/2^+)$	3493.1	2875.1
677.5(5)	4.6(18)	$(25/2^+) \rightarrow (23/2^+)$	5452.2	4774.7
681.3(4)	10(3)	$(23/2^+) \rightarrow 21/2^+$	3464.3	2783.0
710.3(5)	<1	$(21/2^-) \rightarrow (21/2^+)$	3493.1	2783.0
712.1(4)	37(7)	$(23/2^-) \rightarrow 21/2^+$	3495.1	2783.0
726.7(4)	0.8(4)	$\rightarrow (19/2^+)$	3893.9	3167.2
805.7(6)	0.5(2)	$(21/2^+) \rightarrow$	4349.8	3544.3
813.0(3)	3.7(18)	$(37/2^+) \rightarrow (35/2^+)$	7629.7	6816.7
831.2(4)	3.5(17)	$(19/2^+) \rightarrow (15/2^+)$	2875.1	2043.8
851.7(5)	2.1(10)	$(27/2^+) \rightarrow (23/2^+)$	5626.5	4774.7
859.7(6)	0.7(3)	$(15/2^+) \rightarrow 11/2^+$	2043.8	1184.4
890.0(4)	62(9)	$21/2^+ \rightarrow 17/2^+$	2783.0	1893.0
911.7(4)	21(5)	$(27/2^-) \rightarrow (23/2^-)$	4406.8	3495.1
927.2(5)	1.6(8)	$(27/2^+) \rightarrow$	5626.5	4699.6
982.2(4)	2.5(12)	$(19/2^+) \rightarrow 17/2^+$	2875.1	1893.0
1085.6(4)	1.5(7)	$(31/2^-) \rightarrow (27/2^-)$	5492.2	4406.8
1102.5(5)	<1	$(25/2^+) \rightarrow (21/2^+)$	5452.2	4349.8
1130.5(4)	1.8(9)	$\rightarrow (25/2^+)$	6228.7	5098.2
1184.4(4)	100(15)	$11/2^+ \rightarrow 7/2^+$	1184.4	0.0
1206.5(4)	1.8(9)	$\rightarrow (21/2^-)$	4699.6	3493.1
1219.4(4)	1.9(9)	$(27/2^+) \rightarrow (27/2^-)$	5626.5	4406.8
1274.3(4)	3.7(18)	$(19/2^+) \rightarrow 17/2^+$	3167.2	1893.0
1281.9(4)	2.1(10)	$(23/2^+) \rightarrow (21/2^-)$	4774.7	3493.1
1409.3(4)	2.5(12)	$(19/2^-) \rightarrow 17/2^+$	3302.3	1893.0
1448.5(5)	1.6(8)	$(29/2^+) \rightarrow (27/2^-)$	5855.0	4406.8
1495.7(6)	1.3(6)	$(19/2^+) \rightarrow 15/2^+$	3167.2	1671.2
1532.6(5)	2.1(10)	$\rightarrow (29/2^-)$	6554.2	5021.6
1566.7(5)	8.9(27)	$(21/2^+) \rightarrow 21/2^+$	4349.8	2783.0
1651.3(7)	0.5(2)	$\rightarrow 17/2^+$	3544.3	1893.0
1957.2(7)	1.4(7)	$(25/2^+) \rightarrow (23/2^-)$	5452.2	3495.1
1964.3(8)	1.7(9)	$\rightarrow (23/2^-)$	5459.4	3495.1
2397(1)	3.0(15)	$(19/2^+) \rightarrow 17/2^+$	4290	1893.0

[a]The number in parentheses is the error in the last digit.
[b]The relative intensities are normalized to $I_\gamma(1184) = 100$.

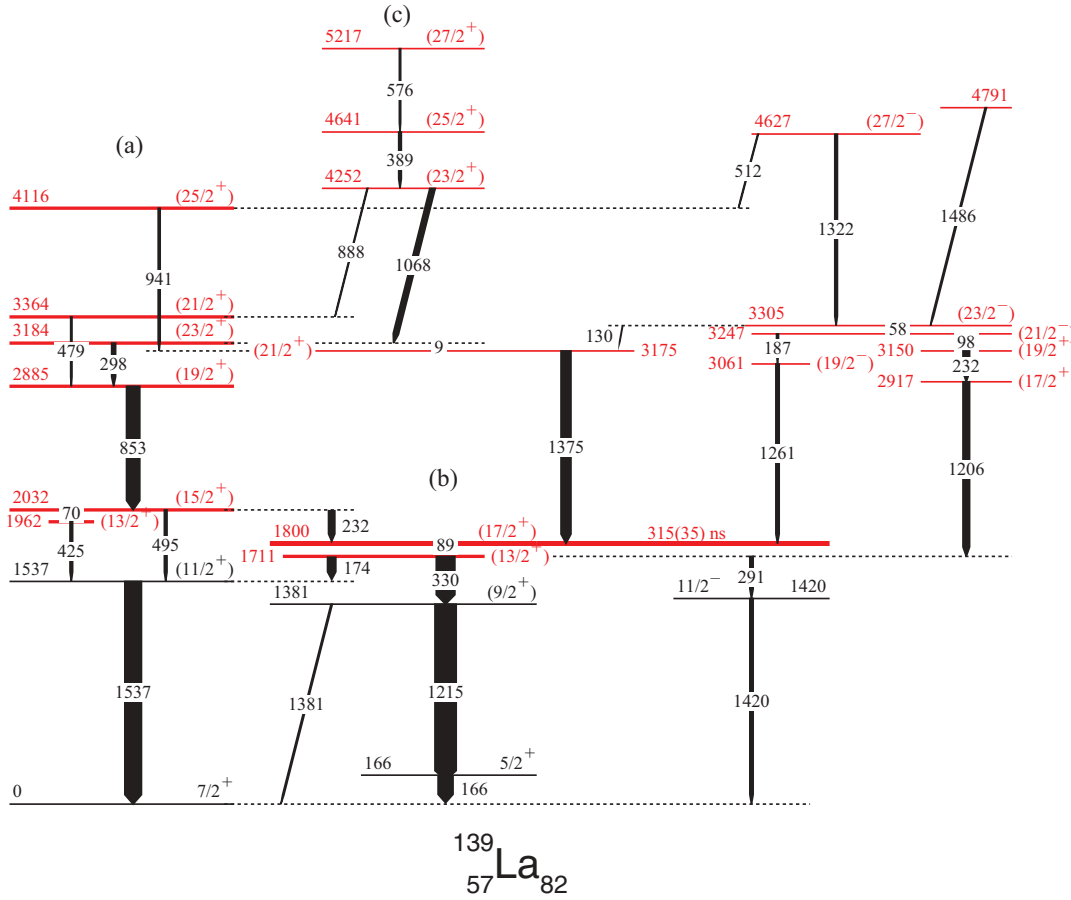

FIG. 3. (Color online) Level scheme of ^{139}La established in this work. The colored states are new. The width of the arrows is indicative of the γ-ray intensity (see text).

reconciled and two states very close in energy do exist in ^{139}La. The 1420-keV state identified in the present work only decays toward the ground state, but a weak decay to the 166-keV state cannot be excluded when taking into account the low intensity measured for the 1420-keV line. In Fig. 3, we have chosen the value $I^{\pi} = 11/2^{-}$, as discussed below.

Noteworthy is the fact that the 232-keV transition has to be a doublet in order to satisfy all its coincidence relationships; the first member is located above the 1800-keV state and the second one above the 2917-keV state. Some examples of double-gated spectra showing the most intense ^{139}La transitions are displayed in Fig. 4.

By using the data from the SAPhIR experiment, the three cascades involved in the decay of the 1800-keV level have been found to be delayed. The time distribution between the detection of two fragments by SAPhIR and of the 1215- or the 330-keV transition by Euroball is shown in Fig. 5. In order to reduce the background, we have selected the events containing an additional γ ray belonging to the 330-1215-166 cascade. Thus the half-life of the 1800-keV level has been obtained, $T_{1/2} = 315(35)$ ns.

The level scheme of ^{139}La includes five transitions with an energy lower than 100 keV. We have observed all their γ lines but the 9- and the 58-keV transitions. The former is located between the levels at 3184 and 3175 keV because of some coincidence relationships. Indeed the spectrum gated by the 1068- and 389-keV lines exhibits both the 1375-keV transition and the 298/853-keV cascade [see Fig. 4(c)], while the spectrum gated by 1322- and 130-keV lines only exhibits the 1375-keV transition. For the 58-keV transition, it is needed to account for all the coincidence relationships of the 1322- and 1486-keV transitions.

The determination of the transition intensities is rather delicate because of the isomeric state at 1800 keV, which induces a loss in intensity $\sim$50% for many transitions in the gated spectra, while some others keep their relative intensity, as they belong to decay paths bypassing the isomeric state. Therefore we do not give any intensity value in Table III. On the other hand, the deexcitation branching ratios of levels, if any, can be determined as they do not suffer the drawback mentioned above; they are given in Table IV.

Angular correlations of transitions emitted by ^{139}La could not be measured due to their too-weak intensities in the (O + Pb) experiment. Spin and parity assignments have been therefore deduced by using the following arguments: (i) The spin values increase with excitation energy, (ii) the high-energy (low-energy) transitions likely have an $E2$ ($M1$) character, and (iii) the measured branching ratios as well as the existence or the absence of cross-over transitions place some conditions on the multipolarities. Starting from the two values already

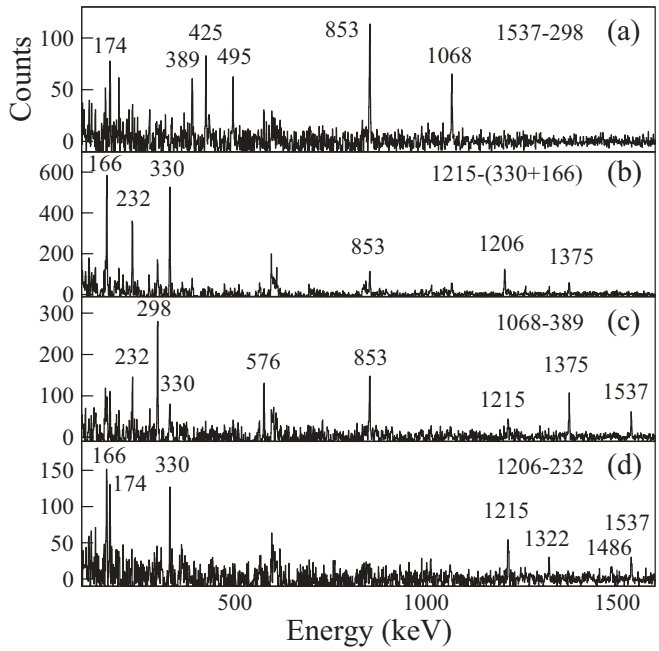

FIG. 4. Examples of double-gated spectra illustrating the most intense ^{139}La transitions.

known, $I^\pi = 7/2^+$ for the ground state and $I^\pi = 5/2^+$ for the first excited state [18], we have obtained the values given in parentheses in Fig. 3; some of them are discussed now.

First of all, it is important to note that the level scheme of ^{139}La does not resemble the one of ^{137}Cs; particularly, its $5/2^+$ state at 166 keV takes part in the yrast structure, while the $5/2^+$ state of ^{137}Cs, being higher in energy (455 keV), is not observed in our work (see Fig. 1). On the other hand, the low-lying part of the level scheme of ^{139}La can be compared to the one of ^{141}Pr, which exhibits both the $5/2^+$ state and the $7/2^+$ one in the in-beam studies [20]. This leads the spin values of the 1381-, 1537- and 1711-keV states to be $9/2^+$,

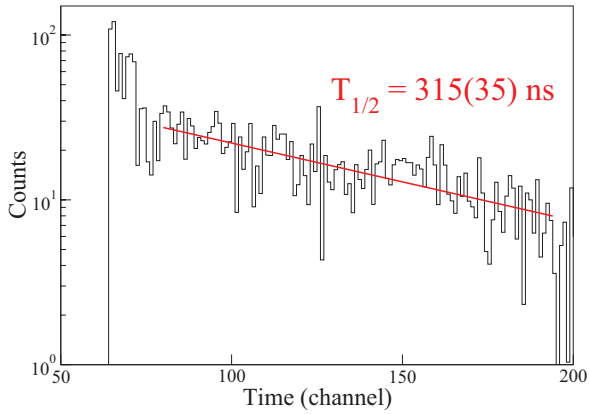

FIG. 5. (Color online) Time distribution between the detection of two fragments by SAPhIR and of a γ transition by Euroball (the γ multiplicity being 2) showing the half-life of the 1800-keV state of ^{139}La: the γ transition is either the 1215- or the 330-keV one; with a gate set on the second γ, which is either the 166-keV or the 330-/1215-keV transition.

TABLE III. Properties of the transitions assigned to ^{139}La observed in this work.

E_γ[a] (keV)	$I_i^\pi \to I_f^\pi$	E_i	E_f
9.0[b]	$(23/2^+) \to (21/2^+)$	3183.7	3174.7
57.7[b]	$(23/2^-) \to (21/2^-)$	3305.0	3247.3
70.0(3)	$(15/2^+) \to (13/2^+)$	2032.1	1962.2
88.7(5)	$(17/2^+) \to (13/2^+)$	1799.8	1711.1
97.6(5)	$(21/2^-) \to (19/2^+)$	3247.3	3149.7
130.3(3)	$(23/2^-) \to (21/2^+)$	3305.0	3174.7
165.6(3)	$5/2^+ \to 7/2^+$	165.6	0.0
174.0(3)	$(13/2^+) \to (11/2^+)$	1711.1	1537.0
186.7(4)	$(21/2^-) \to (19/2^-)$	3247.3	3060.6
232.3(4)	$(15/2^+) \to (17/2^+)$	2032.1	1799.8
232.3(4)	$(19/2^+) \to (17/2^+)$	3149.7	2917.4
291.3(3)	$(13/2^+) \to 11/2^-$	1711.1	1420.0
298.4(3)	$(23/2^+) \to (19/2^+)$	3183.7	2885.3
330.3(3)	$(13/2^+) \to (9/2^+)$	1711.1	1380.8
388.9(3)	$(25/2^+) \to (23/2^+)$	4640.6	4251.7
425.2(3)	$(13/2^+) \to (11/2^+)$	1962.2	1537.0
478.6(4)	$(21/2^+) \to (19/2^+)$	3363.9	2885.3
495.0(3)	$(15/2^+) \to (11/2^+)$	2032.1	1537.0
512(1)	$(27/2^-) \to (25/2^+)$	4627.3	4115.6
576.4(4)	$(27/2^+) \to (25/2^+)$	5217.0	4640.6
853.2(4)	$(19/2^+) \to (15/2^+)$	2885.3	2032.1
887.8(4)	$(23/2^+) \to (21/2^+)$	4251.7	3363.9
940.9(4)	$(25/2^+) \to (21/2^+)$	4115.6	3174.7
1068.0(4)	$(23/2^+) \to (23/2^+)$	4251.7	3183.7
1215.2(5)	$(9/2^+) \to 5/2^+$	1380.8	165.6
1206.3(5)	$(17/2^+) \to (13/2^+)$	2917.4	1711.1
1260.8(5)	$(19/2^-) \to (17/2^+)$	3060.6	1799.8
1322.3(5)	$(27/2^-) \to (23/2^-)$	4627.3	3305.0
1374.9(4)	$(21/2^+) \to (17/2^+)$	3174.7	1799.8
1380.9(6)	$(9/2^+) \to 7/2^+$	1380.8	0.0
1420.0(5)	$11/2^- \to 7/2^+$	1420.0	0.0
1485.6(6)	$\to (23/2^-)$	4790.6	3305.0
1537.0(4)	$(11/2^+) \to 7/2^+$	1537.0	0.0

[a]The number in parentheses is the error in the last digit.
[b]Not observed, inferred from the coincidence relationships.

$11/2^+$, and $13/2^+$, respectively. The $13/2^+$ state of ^{141}Pr also decays to the $11/2^-$ level at 1118 keV. Thus we propose that the 1420-keV state measured in the present work is the $11/2^-$ level already identified in transfer reactions, as the spin value assigned to the other level, observed in the β decay, $I^\pi = 5/2^+$ or $7/2^+$ [18] is too low. For the isomeric state at 1800 keV, we choose $I^\pi = 17/2^+$, assuming that the 89-keV transition is $E2$. This leads to $B(E2; 17/2^+ \to 13/2^+) = 81(9)e^2\text{fm}^4$, i.e., 1.9(2) W.u. The yrast cascades of ^{141}Pr and ^{143}Pm also contain one delayed $E2$ transition which exhibits a similar value of hindrance, 0.87(10) and 1.52(6) W.u., respectively. Nevertheless the spin value of their isomeric states is one unit less, $15/2^+$. This change is due to the number of protons occupying the two orbits close to the Fermi level, namely $\pi g_{7/2}$ and $\pi d_{5/2}$. For the decay of the 3184-keV state of ^{139}La, the fact that a 9-keV transition competes with a 298-keV one implies that the former is $M1$ while the latter has to be hindered, such as is expected for an $E2$ transition of low energy. A similar argument is used for the choice of the parity value of the

TABLE IV. Branching ratios of the states of ^{139}La measured in this work.

State (keV)	E - I_{tot} [a,b] (keV) - (%)	E - I_{tot} [a,b] (keV) - (%)	E - I_{tot} [a,b] (keV) - (%)
1381	1215 - 95(9)	1381 - 5(2)	
1711	174 - 35(6)	291 - 10(3)	330 - 55(8)
2032	70 - 20(4)	232 - 60(8)	495 - 20(4)
3184	298 - 55(8)	9 - 45(7)	
3247	98 - 55(8)	187 - 45(7)	
3305	58 - 70(9)	130 - 30(5)	
4252	888 - 14(3)	1068 - 86(9)	
4627	512 - 10(3)	1322 - 90(9)	

[a]The intensity balances used to measure the branching ratios take into account the conversion electrons of the low-energy transitions.
[b]The number in parentheses is the error in the last digit.

3305-keV level: the 58-keV transition is assumed to be $M1$ while the 130-keV transition would be $E1$, as imposed by their relative branching ratios (Table IV).

B. Study of the even-Z isotones

1. Level scheme of $^{136}_{54}Xe$

The yrast excitations of ^{136}Xe, studied using a ^{248}Cm source, were identified up to an excitation energy of 6.2 MeV and a spin value of (13^+) [4]. Since ^{136}Xe is produced in both reactions used in the present work and the fusion-fission process brings higher angular momenta than that obtained in the spontaneous fission of actinides, we have looked for new γ-ray cascades emitted by ^{136}Xe. The level scheme built from these analyses is shown in Fig. 6. We have gathered in Table V the properties of all the transitions assigned to ^{136}Xe from this work.

The level scheme has been extended up to 7.9 MeV excitation energy by means of several γ rays in cascade. Moreover three new decay paths of the (12^+) state at 5950 keV have been observed. The spin values of states lying below 2.3 MeV excitation energy are those proposed in the previous works [18]. In addition we have measured the angular correlations of a few γ rays of ^{136}Xe lying above its long-lived isomeric state (see Table VI). The results indicate that the 968- and 255-keV transitions have an $E2$ character, knowing that the 370-keV γ-ray is a dipole transition linking two states having the same spin value [18]. It has to be noticed that a new γ ray linking the 2261-keV level to the 4^+ state at 1694 keV has been observed, which is in good agreement with the involved spin values. Finally, the 2866-keV state has $I^\pi = 8^+$, as it is directly populated by a 10^+ state and it decays toward a 6^+ state (see Fig. 6). For the highest-spin part, we have assumed that the spin values increase with excitation energy and that the low-energy transitions have an $M1$ character.

We have looked for isomeric states in ^{136}Xe by using the data registered with the SAPhIR detector. Only one γ-ray cascade has been found to be delayed, that decaying the known isomeric state at 1891 keV.

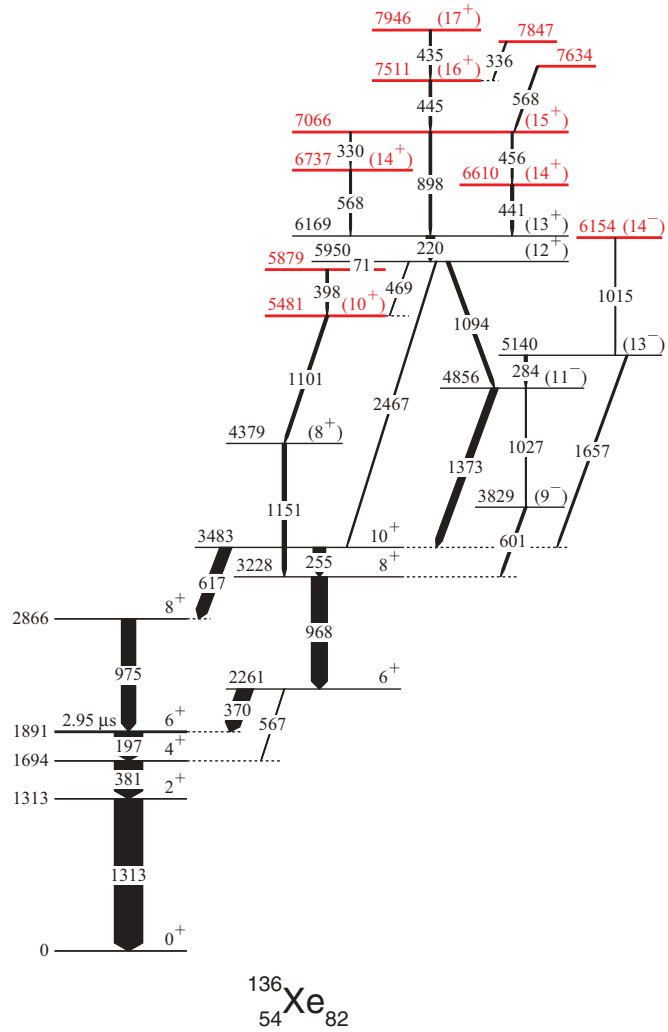

FIG. 6. (Color online) Level scheme of ^{136}Xe established in this work. The colored states are new. The width of the arrows is proportional to the γ-ray intensity. The half-life value of the 6^+_1 state is from Ref. [18].

2. Level scheme of $^{138}_{56}Ba$

Previous information regarding the medium-spin states of ^{138}Ba comes from results of the $(\alpha,2n)$ reaction, where levels with spin values up to $12\hbar$ and excitation energies of 4.7 MeV were identified [21]. All the yrast levels have been confirmed by the analyses of both data sets of the present work. Moreover, the spectra doubly-gated on the known transitions allowed us to identify many new γ lines which extend the level scheme up to 9.3 MeV excitation energy. We have gathered in Table VII the properties of all the transitions assigned to ^{138}Ba from this work and its level scheme is drawn in Fig. 7.

First, several transitions have been found to populate the 12^+ state at 4687 keV. The most intense is the 705-keV transition [see the spectrum of Fig. 8(a)] which defines the new level at 5392 keV. Above it, the gamma intensity is spread over several lines. Second, a new structure has been built above the 9^- state already known from the $(\alpha,2n)$ reaction (see the right part of Fig. 7). Third, the high-energy part of the yrast structure of ^{138}Ba consists of ten transitions in mutual coincidences

TABLE V. Properties of the transitions assigned to ^{136}Xe observed in this experiment.

E_γ [a] (keV)	I_γ [a,b]	$I_i^\pi \rightarrow I_f^\pi$	E_i	E_f
70.7[c]	6.2(19)[d]	$(12^+)\rightarrow(11^+)$	5949.5	5878.8
196.8(3)		$6^+ \rightarrow 4^+$	1890.8	1694.0
219.5(3)	29(6)	$(13^+) \rightarrow (12^+)$	6169.0	5949.5
254.6(3)	44(7)	$10^+ \rightarrow 8^+$	3482.8	3228.1
284.0(4)	8.8(26)	$(13^-) \rightarrow (11^-)$	5139.8	4855.8
329.8(4)	7(2)	$(15^+) \rightarrow (14^+)$	7066.3	6736.5
336.4(4)	3.4(14)	$\rightarrow (16^+)$	7847.2	7510.8
369.7(3)	53(8)	$6^+ \rightarrow 6^+$	2260.5	1890.8
381.2(2)		$4^+ \rightarrow 2^+$	1694.0	1312.8
398.2(4)	7.8(23)	$(11^+) \rightarrow (10^+)$	5878.8	5480.6
435.4(4)	5.1(15)	$(17^+) \rightarrow (16^+)$	7946.2	7510.8
441.2(3)	10(3)	$(14^+) \rightarrow (13^+)$	6610.3	6169.0
444.5(4)	8.5(25)	$(16^+) \rightarrow (15^+)$	7510.8	7066.3
455.9(4)	7(2)	$(15^+) \rightarrow (14^+)$	7066.3	6610.3
469.1(5)	1.6(8)	$(12^+) \rightarrow (10^+)$	5949.5	5480.6
567.0(5)	3(2)	$6^+ \rightarrow 4^+$	2260.5	1694.0
567.5(5)	7(2)	$(14^+) \rightarrow (13^+)$	6736.5	6169.0
568.0(5)	7(2)	$\rightarrow (15^+)$	7634.3	7066.3
600.8(4)	8(3)	$(9^-) \rightarrow 8^+$	3828.9	3228.1
617.0(3)	39(6)	$10^+ \rightarrow (8^+)$	3482.8	2865.9
897.5(4)	7(2)	$(15^+) \rightarrow (13^+)$	7066.3	6169.0
967.6(3)	56(8)	$8^+ \rightarrow 6^+$	3228.1	2260.5
975.1(3)	47(7)	$(8^+) \rightarrow 6^+$	2865.9	1890.8
1014.6(4)	6(3)	$(14^-) \rightarrow (13^-)$	6154.4	5139.8
1027.1(4)	4(2)	$(11^-) \rightarrow (9^-)$	4855.8	3828.9
1093.7(3)	11(3)	$(12^+) \rightarrow (11^-)$	5949.5	4855.8
1101.3(3)	9.7(29)	$(10^+) \rightarrow (8^+)$	5480.6	4379.3
1151.2(3)	13(3)	$(8^+) \rightarrow 8^+$	4379.3	3228.1
1312.8(2)		$2^+ \rightarrow 0^+$	1312.8	0.0
1373.0(4)	23(5)	$(11^-) \rightarrow 10^+$	4855.8	3482.8
1657.0(5)	6(3)	$(13^-) \rightarrow 10^+$	5139.8	3482.8
2467.2(5)	5.0(25)	$(12^+) \rightarrow 10^+$	5949.5	3482.8

[a]The number in parentheses is the error in the last digit.
[b]The relative intensities are normalized to the sum of the populations of the 6_1^+ isomeric state, $I_\gamma(370) + I_\gamma(975) = 100$.
[c]Not observed, inferred from the coincidence relationships.
[d]This number is $I_{\rm tot}$and not I_γ.

which are located between 5740 and 9333 keV. The first three states of this new band show many decay paths involving states lying in the excitation-energy range 3620–5357 keV, indicating a large change of configuration, which will be discussed in Sec. IV.

For the spin assignments, we have first used the results of the previous experiment [21], particularly the angular distributions

TABLE VI. Coincidence rates between a few γ rays of ^{136}Xe lying above its long-lived isomeric state, as a function of their relative angle of detection, normalized by the ones obtained around 75°.

γ-γ coincidence	$R(22°)$[a]	$R(46°)$[a]	$R(75°)$[a]
968 - 370	1.5(3)	1.2(1)	1.00(6)
255 - 968	1.2(1)	1.0(1)	1.00(5)

[a]The number in parentheses is the error in the last digit.

TABLE VII. Properties of the transitions assigned to ^{138}Ba observed in this work.

E_γ [a] (keV)	I_γ [a,b]	$I_i^\pi \rightarrow I_f^\pi$	E_i	E_f
112.1(5)	27(5)	$6^+ \rightarrow 6^+$	2201.4	2089.3
183.7(5)	3.3(13)	$(12^+) \rightarrow (11^+)$	5923.7	5740.1
191.5(3)		$6^+ \rightarrow 4^+$	2089.3	1897.8
239.0(4)	2.2(10)	$(15^+) \rightarrow (14^+)$	7225.9	6986.9
285.4(3)	12(4)	$(13^+) \rightarrow (12^+)$	6209.0	5923.7
288.2(3)	12(4)	$10^+ \rightarrow 10^+$	3908.6	3620.3
301.4(4)	4.4(18)	$(18^+) \rightarrow (17^+)$	8280.1	7978.7
306.1(3)	7.3(22)	$(16^+) \rightarrow (15^+)$	7532.0	7225.9
396.1(5)	2.1(10)	$(20^+) \rightarrow (19^+)$	9332.6	8936.5
438.3(3)	40(6)	$10^+ \rightarrow 8^+$	3620.3	3182.0
446.7(3)	7.4(22)	$(14^+) \rightarrow (13^+)$	6655.7	6209.0
446.7(5)	5.6(17)	$(17^+) \rightarrow (16^+)$	7978.7	7532.0
449.1(3)	9.6(29)	$9^- \rightarrow 8^+$	3631.1	3182.0
462.4(3)		$4^+ \rightarrow 2^+$	1897.8	1435.4
481.8(3)	8.3(25)	$(13^-) \rightarrow (11^-)$	5184.2	4702.4
516.7(4)	3.2(13)	$5^+ \rightarrow 4^+$	2414.5	1897.8
527.4(4)	6.9 (20)	$(14^-) \rightarrow (13^-)$	5919.6	5392.2
567.3(3)	6.1(18)	$(12^+) \rightarrow$	5923.7	5356.8
570.1(3)	7.1(21)	$(15^+) \rightarrow (14^+)$	7225.9	6655.7
656.4(5)	3.2(15)	$(19^+) \rightarrow (18^+)$	8936.5	8280.1
705.2(3)	23(5)	$(13^-) \rightarrow 12^+$	5392.2	4687.0
726.7(3)	35(7)	$10^+ \rightarrow 8^+$	3908.6	3182.0
778.0(4)	5.4(19)	$(14^+) \rightarrow (13^+)$	6986.9	6209.0
778.4(3)	41(6)	$12^+ \rightarrow 10^+$	4687.0	3908.6
797.1(4)	3.0(15)	$(12^+) \rightarrow$	5923.7	5126.6
804.2(3)	9.4(28)	$(15^-) \rightarrow (13^-)$	6196.4	5392.2
837.8(4)	5.1(18)	$(16^-) \rightarrow (14^-)$	6757.4	5919.6
856.9(5)	2.4(12)	$\rightarrow (17^-)$	8010.7	7153.8
944.0(5)	1.7(8)	$(7^+) \rightarrow 5^+$	3358.5	2414.5
957.4(5)	3.1(15)	$(17^-)\rightarrow (15^-)$	7153.8	6196.4
980.3(3)	23(5)	$8^+ \rightarrow 6^+$	3182.0	2201.4
1067.1(5)	3.5(15)	$(14^+) \rightarrow (14^-)$	6986.9	5919.6
1071.3(3)	7.8(23)	$(11^-) \rightarrow 9^-$	4702.4	3631.1
1082.1(3)	7.8(23)	$(11^-) \rightarrow 10^+$	4702.4	3620.3
1092.7(3)	73(11)	$8^+ \rightarrow 6^+$	3182.0	2089.3
1205.2(5)	2(1)	$\rightarrow (15^-)$	7401.6	6196.4
1221.2(5)	2.7(13)	$(12^+) \rightarrow (11^-)$	5923.7	4702.4
1236.4(4)	6.0(18)	$(12^+) \rightarrow 12^+$	5923.7	4687.0
1435.4(4)		$2^+ \rightarrow 0^+$	1435.4	0.0
1506.3(5)	2.4(12)	$\rightarrow 10^+$	5126.6	3620.3
1521.9(5)	4.2(15)	$(13^+) \rightarrow 12^+$	6209.0	4687.0
1736.4(5)	4.9(17)	$\rightarrow 10^+$	5356.8	3620.3
1802.6(6)	2.9(14)	$(14^+) \rightarrow (13^-)$	6986.9	5184.2
2119.8(8)	2.1(10)	$(11^+) \rightarrow 10^+$	5740.1	3620.3
2303.6(8)	1.4(7)	$(12^+) \rightarrow 10^+$	5923.7	3620.3

[a]The number in parentheses is the error in the last digit.
[b]The relative intensities are normalized to the sum of the populations of the 6_1^+ isomeric state, $I_\gamma(112) + I_\gamma(1093) = 100$.

and linear polarizations. It is worth mentioning that the (α,2n) reaction populates both yrast and yrare states of the produced nuclei. Thus in many cases, the knowledge of the transition multipolarity was not enough to determine unambiguously the spin and parity values of the decaying state. For instance, even though the multipolarity of the 449-keV transition was

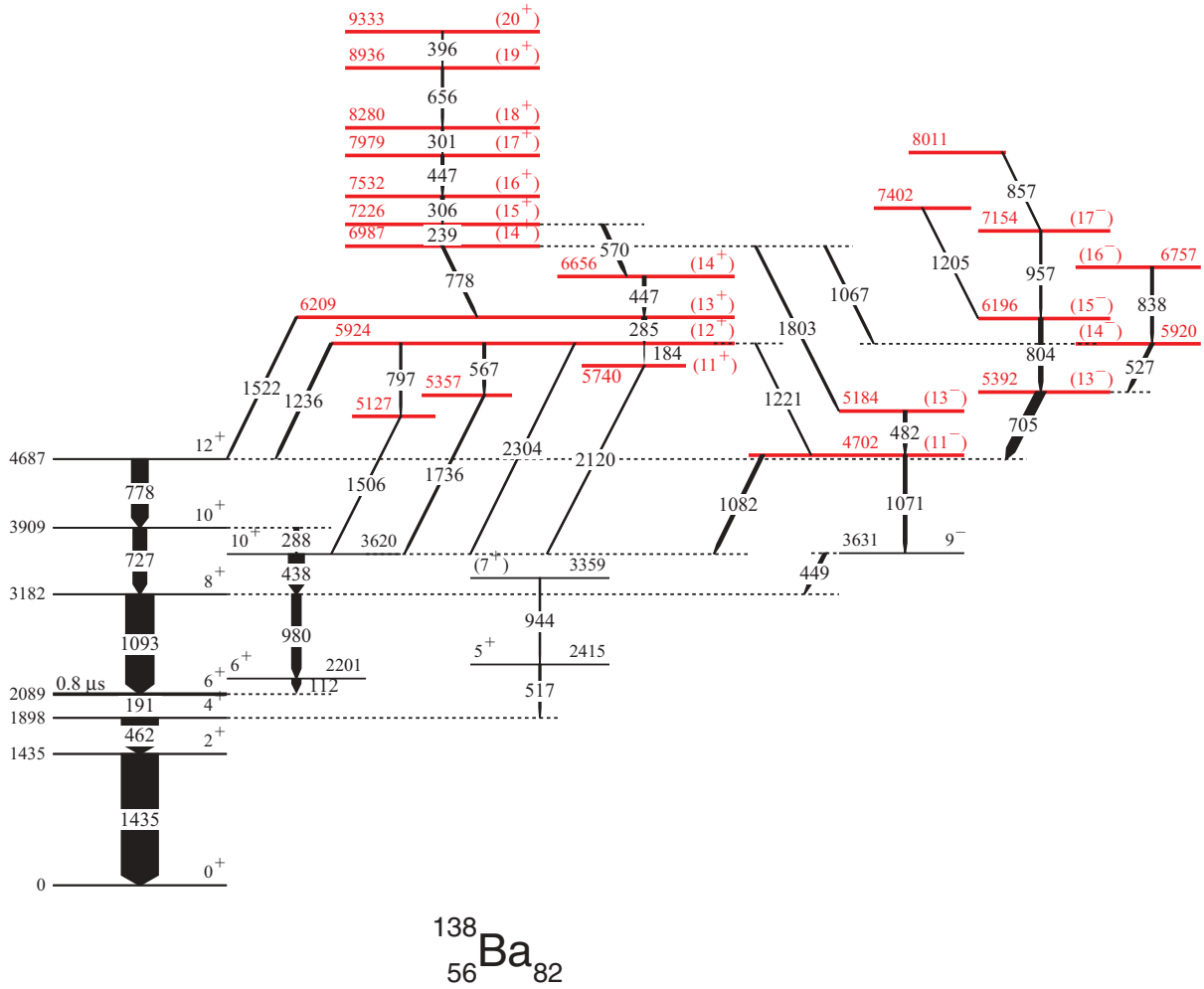

FIG. 7. (Color online) Level scheme of ^{138}Ba established in this work. The colored states are new. The width of the arrows is proportional to the γ-ray intensity. The half-life value of the 6^+ state is from Ref. [18].

measured to be stretched $E1$ (see Table II of Ref. [21]), the authors had given the spin value of the 3631-keV level with parentheses, $I^\pi = (9^-)$, because $I^\pi = 7^-$ could not be excluded. Since in the fusion-fission reactions the yrast states are the most populated, the spin value of the 3631-keV level cannot be 7^- but is 9^-, without ambiguity. The same arguments hold for the 3909-keV level ($I^\pi = 10^+$) and 4687-keV level ($I^\pi = 12^+$), as the 727- and the 778-keV γ rays are stretched $E2$ transitions (see Table II of ref. [21]).

The first three states of the high-energy part of the yrast structure of ^{138}Ba are proposed to have $I^\pi = (11^+)$, (12^+), and (13^+) respectively, that are consistent with their links to the 10^+_1 and 12^+_1 states, assuming that the spin values increase with excitation energy and that the low-energy transitions have an $M1$ character. Then the 4702-keV state is (11^-), since it is populated by the (12^+) state at 5924 keV and it decays toward the 9^- state at 3631 keV and the 10^+ state at 3620 keV. Finally, assuming that all the transitions located above the 6209-keV levels have a $M1$ multipolarity, we assign $I^\pi = (20^+)$ to the 9333-keV level.

We have looked for isomeric states in ^{138}Ba by using the data registered with the SAPhIR detector. Only one γ-ray cascade has been found to be delayed, that decaying the known isomeric state at 2089 keV (see Fig. 7). The spectrum of γ rays which have been detected in the time interval 50 ns – 1 μs after the detection of two fragments by SAPhIR and in coincidence with the 1435-keV line is shown in Fig. 9. In addition to the expected 462- and 191-keV transitions belonging to the known delayed cascade, we observe a small peak at 180 keV. The latter is emitted by one of the complementary fragments, ^{101}Mo, which also exhibits an isomeric state with $T_{1/2} = 95(15)$ ns [22]. Such a spectrum demonstrates the selectivity of an apparatus such as SAPhIR plus Euroball when looking for the decay of isomeric states of the fission fragments.

3. *Level scheme of $^{140}_{58}$Ce*

$^{140}_{58}$Ce is the heaviest $N = 82$ isotone obtained in the fusion-fission reactions used in the present work. Since it is in the light-A tail of the Ce fragment distribution, its population is unfortunately low. Nevertheless we have identified several new high-spin states located above the 13^- state at 5102 keV, which was the highest-spin level obtained in the $(\alpha,2n)$ reaction [23].

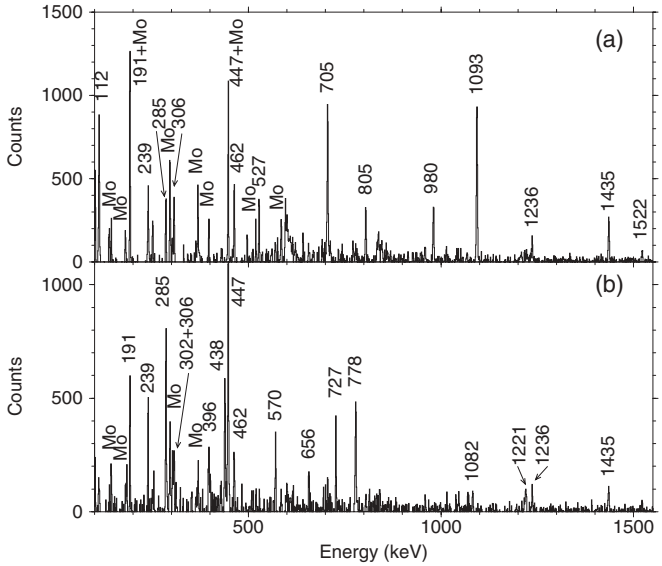

FIG. 8. Spectra of γ rays in coincidence with two transitions of ^{138}Ba: (a) with the 727- and the 778-keV transitions; (b) with the 1093- and the 570- or 306-keV transitions. Transitions emitted by $^{101-104}$Mo, the complementary fragments of ^{138}Ba, are labeled by Mo.

Most of the new states have likely a negative parity, as they are only linked to the 13^- state.

All the levels observed in this work are drawn in Fig. 10. Those lying below 5200 keV are the same as the yrast states previously obtained in the $(\alpha,2n)$ reaction, their spin and parity values being determined from results of angular distributions and linear polarizations [23]. The properties of the transitions observed in the present work are gathered in Table VIII. Even though most of them were already known from the previous work, they are repeated here for completeness. For the spin assignments of the new levels, we have used the same arguments as those given in the previous sections. Lastly, we have looked for isomeric states in ^{140}Ce by using the data registered with the SAPhIR detector. Only the γ rays decaying the two known isomeric states at 2108 keV and 3714 keV (see Fig. 10) are weakly observed.

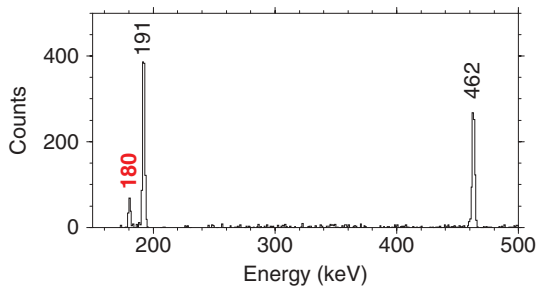

FIG. 9. (Color online) Spectrum of γ rays which have been detected in the time interval 50 ns – 1 μs after the detection of two fragments by SAPhIR and in coincidence with the 1435-keV line of ^{138}Ba. The 180-keV transition is emitted by the isomeric state of ^{101}Mo, partner of ^{138}Ba in the C + U fusion-fission reaction.

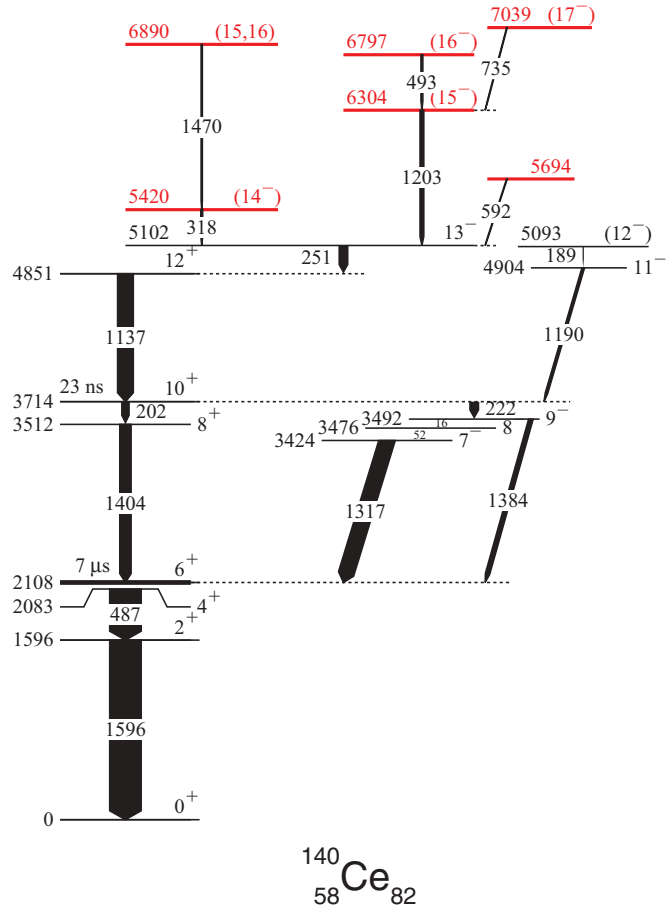

FIG. 10. (Color online) Level scheme of ^{140}Ce established in this work. The colored states are new. The width of the arrows is proportional to the γ-ray intensity. The half-life values of the 6^+ and 10^+ states are from Ref. [18].

IV. DISCUSSION

The high-spin level schemes of the $N = 82$ isotones with $Z > 50$ are expected to involve only the three high-j orbits, $\pi g_{7/2}$, $\pi d_{5/2}$, and $\pi h_{11/2}$. The two former being very close to the Fermi level for $Z \leqslant 58$, positive-parity structures dominate the low-energy part of the spectra of the isotones studied in the present work. In this section, we present general features of their high-spin behaviors, particularly the maximum spin values which can be obtained when all the proton pairs are broken; we discuss the breaking of one proton pair for some simple configurations and we point out the main differences which may occur in the odd-Z isotones; we compare the results of shell-model calculations to the experimental levels; and last we show that the excitation of the $N = 82$ core is the only way to get the highest-spin values of the lightest $N = 82$ isotones.

A. General features

Simple excitation modes are expected in the $N = 82$ isotones lying just above the doubly-magic ^{132}Sn because of the low number of available proton orbits. Being close in energy, the first two orbits, $\pi g_{7/2}$ and $\pi d_{5/2}$, can be assumed

TABLE VIII. Properties of the transitions assigned to ^{140}Ce observed in this work.

E_γ[a] (keV)	I_γ[a,b]	$I_i^\pi \rightarrow I_f^\pi$	E_i	E_f
16[c]		$9^- \rightarrow 8^-$	3491.8	3476
24.5[c]		$6^+ \rightarrow 4^+$	2107.6[d]	2083
52(1)		$8^- \rightarrow 7^-$	3476	3424.4
188.9(5)	4(2)	$(12^-) \rightarrow 11^-$	5093.1	4904.2
202.0(3)	28(6)	$10^+ \rightarrow 8^+$	3713.9	3512.0
222.0(3)	52(8)	$10^+ \rightarrow 9^-$	3713.9	3491.8
250.9(3)	33(7)	$13^- \rightarrow 12^+$	5101.6	4850.7
318.0(4)	5.8(17)	$(14^-) \rightarrow 13^-$	5419.6	5101.6
487(1)[e]		$4^+ \rightarrow 2^+$	2083	1596
493.0(4)	6.4(20)	$(16^-) \rightarrow (15^-)$	6797.2	6304.2
592.3(5)	4(2)	$\rightarrow 13^-$	5693.9	5101.6
734.6(5)	4(2)	$(17^-) \rightarrow (15^-)$	7038.8	6304.2
1136.8(3)	51(8)	$12^+ \rightarrow 10^+$	4850.7	3713.9
1190.3(4)	8.8(25)	$11^- \rightarrow 10^+$	4904.2	3713.9
1202.6(3)	13(3)	$(15^-) \rightarrow 13^-$	6304.2	5101.6
1316.8(3)	51(8)	$7^- \rightarrow 6^+$	3424.4	2107.6[d]
1384.2(3)	14(4)	$9^- \rightarrow 6^+$	3491.8	2107.6[d]
1404.4(3)	35(8)	$8^+ \rightarrow 6^+$	3512.0	2107.6[d]
1470.2(7)	4.3(17)	$(15,16) \rightarrow (14^-)$	6889.8	5419.6
1596(1)[e]		$2^+ \rightarrow 0^+$	1596	0.0

[a]The number in parentheses is the error in the last digit.
[b]The relative intensities are normalized to the sum of the populations of the 6_1^+ isomeric state, $I_\gamma(1405) + I_\gamma(1317) + I_\gamma(1385) = 100$.
[c]Not observed in the present work, from Ref. [23].
[d]Excitation energy from Ref. [23].
[e]Transition having a very weak intensity in this experiment because of the long half-life of the 6^+ state.

to be filled together, thus the configurations are written as $(\pi g_{7/2}\pi d_{5/2})^n$, instead of $(\pi g_{7/2})^i(\pi d_{5/2})^j$, with $i + j = n$. The maximum value of angular momentum, which can be achieved when proton pairs are broken, depends on the total number of valence protons. For $^{134}_{52}$Te, the breaking of the proton pair gives $I^\pi_{\max} = 6^+$, while one gets the very maximum value, $I^\pi = 25/2^+$, for mid-occupation of the two orbits in $^{139}_{57}$La. Noteworthy is the fact that, due to the presence of two different orbits, the same value of $I^\pi_{\max}$ is obtained for two different configurations of the even-Z isotones, such as 6^+ for $(\pi g_{7/2})^2$ and $(\pi g_{7/2})^1(\pi d_{5/2})^1$, or 10^+ for $(\pi g_{7/2})^3(\pi d_{5/2})^1$ and $(\pi g_{7/2})^2(\pi d_{5/2})^2$, meaning that we expect two 6^+ states or two 10^+ states in the corresponding nuclei.

The maximum values of angular momentum obtained for the complete alignment of the angular momenta of the protons lying in the $\pi g_{7/2}$ and $\pi d_{5/2}$ orbits are given in the first part of Table IX, for the $N = 82$ isotones with $52 \leqslant Z \leqslant 58$. These values are well below the ones which have been observed in the present work. The promotion of one proton in the $\pi h_{11/2}$ orbit leads to higher values of angular momenta as well as a change of parity (see the second part of Table IX). One can remark that some negative-parity structures observed in ^{136}Xe, ^{137}Cs, and ^{138}Ba agree with these quoted values of $I^\pi_{\max}$. Finally the values of $I^\pi_{\max}$ are increased by $10\hbar$ when a proton pair occupying the $\pi h_{11/2}$ orbit is broken (see the last part of Table IX). Nevertheless such a process is expected at high

TABLE IX. Maximum values of angular momentum obtained from various configurations with several broken proton pairs, expected in the $N = 82$ isotones with $52 \leqslant Z \leqslant 58$. The degeneracy, d, is the number of the configurations $(\pi g_{7/2})^i(\pi d_{5/2})^j$, $i + j = n$, leading to the same value of $I^\pi_{\max}$.

Configuration	$I^\pi_{\max}$	d	Nucleus
$(\pi g_7\pi d_5)^n$			
$n = 2$	6^+	2	^{134}Te, ^{136}Xe, ^{138}Ba, ^{140}Ce
$n = 3$	$17/2^+$	1	^{135}I, ^{137}Cs, ^{139}La
$n = 4$	10^+	2	^{136}Xe, ^{138}Ba, ^{140}Ce
$n = 5$	$23/2^+$	1	^{137}Cs, ^{139}La
$n = 6$	12^+	2	^{138}Ba, ^{140}Ce
$n = 7$	$25/2^+$	1	^{139}La
$(\pi g_7\pi d_5)^n(\pi h_{11})^1$			
$n = 1$	9^-	1	^{134}Te, ^{136}Xe, ^{138}Ba, ^{140}Ce
$n = 2$	$23/2^-$	2	^{135}I, ^{137}Cs, ^{139}La
$n = 3$	14^-	1	^{136}Xe, ^{138}Ba, ^{140}Ce
$n = 4$	$31/2^-$	2	^{137}Cs, ^{139}La
$n = 5$	17^-	1	^{138}Ba, ^{140}Ce
$n = 6$	$35/2^-$	2	^{139}La
$n = 7$	18^-	1	^{140}Ce
$(\pi g_7\pi d_5)^n(\pi h_{11})^2$			
$n = 1$	$27/2^+$	1	^{135}I, ^{137}Cs, ^{139}La
$n = 2$	16^+	2	^{136}Xe, ^{138}Ba ^{140}Ce
$n = 3$	$37/2^+$	1	^{137}Cs, ^{139}La
$n = 4$	20^+	2	^{138}Ba, ^{140}Ce
$n = 5$	$43/2^+$	1	^{139}La
$n = 6$	22^+	2	^{140}Ce

excitation energy in the nuclei of interest, since that orbit is located far from their Fermi levels.

Neutron excitation across the $N = 82$ gap was proposed to be involved in the highest-spin part of the yrast band of ^{134}Te, ^{135}I, and ^{136}Xe [3,4]. The gain in angular momentum is 9^+ for the $(\nu h_{11/2})^{-1}(\nu f_{7/2})^{+1}$ excitation. While such an excitation is much more favorable for $Z = 52$–54 than the breaking of a $\pi h_{11/2}$ pair mentionned above, it has not to be excluded for higher Z values. Indeed two excited states of ^{137}Cs lying at 4.35 and 4.77 MeV were related to the excitation of the $N = 82$ core [5]. The clues of neutron excitation across the $N = 82$ gap will be presented in Sec. IV C and discussed in Sec. IV D, using the experimental results obtained in the present work.

B. Breaking of one proton pair

The *first* breaking of a proton pair in the $N = 82$ isotones having $52 \leqslant Z \leqslant 58$ gives rise to different multiplets which depend on the total number of protons occupying the $\pi g_{7/2}$ and $\pi d_{5/2}$ orbits.

In the even-Z isotones, we expect two simple configurations having a broken pair, $(\pi g_{7/2})^2$ and $(\pi g_{7/2})^1(\pi d_{5/2})^1$, the remaining protons lying as pairs in the $\pi g_{7/2}$ or/and $\pi d_{5/2}$ orbit according to the Pauli principle. Both configurations lead to $I^\pi_{\max} = 6^+$. These two 6^+ states were identified in ^{134}Te, ^{136}Xe, ^{138}Ba, and ^{140}Ce [3,4,21,23]. Their excitation energies evolve as a function of the position of the proton Fermi level within the two orbits, as shown in Fig. 11 (see the filled circles).

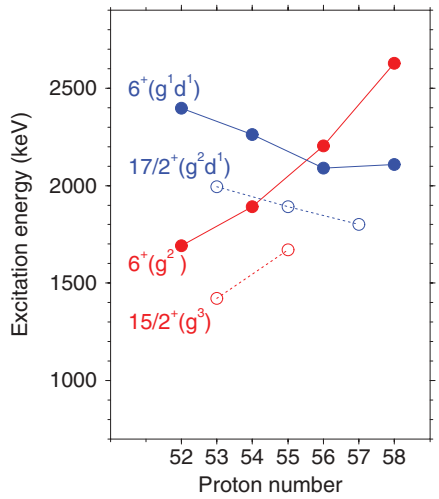

FIG. 11. (Color online) Evolution of the experimental two 6^+ states in the even-Z isotones and of the $15/2_1^+$ and $17/2_1^+$ states in the odd-Z isotones (data from this work and ref. [18]).

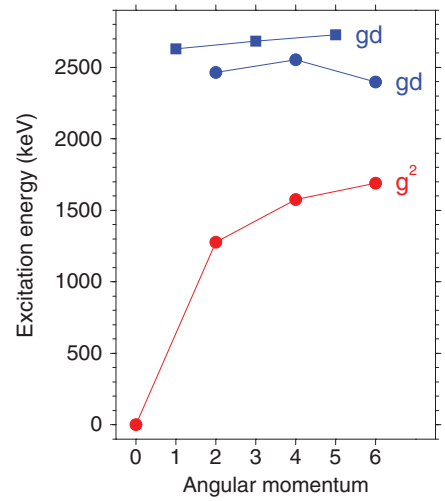

FIG. 12. (Color online) Experimental level scheme of ^{134}Te showing the states issued from the $(\pi g_{7/2})^2$ and $(\pi g_{7/2})^1(\pi d_{5/2})^1$ configurations [18], with even values of angular momentum (circles) and odd ones (squares).

The case of the odd-Z isotones is more delicate. If the odd proton is located in the $\pi g_{7/2}$ orbit, the *first* breaking of a $(\pi g_{7/2})^2$ pair leads to the $(\pi g_{7/2})^3$ configuration, with $I^\pi_{\max} = 15/2^+$. When the odd proton is promoted to the $\pi d_{5/2}$ orbit, the multiplet of the $(\pi g_{7/2})^2(\pi d_{5/2})^1$ configuration extends up to $I^\pi_{\max} = 17/2^+$. First, it is interesting to notice the similar behaviors of the $I^\pi_{\max}$ states of the odd-Z and even-Z isotones: the $15/2^+$ level of $(\pi g_{7/2})^3$ and the 6^+ level of $(\pi g_{7/2})^2$ on the one hand, the $17/2^+$ level of $(\pi g_{7/2})^2(\pi d_{5/2})^1$ and the 6^+ level of $(\pi g_{7/2})^1(\pi d_{5/2})^1$ on the other hand (see Fig. 11). Second, it is worth noting that large changes in the structure of the $(\pi g_{7/2})^2(\pi d_{5/2})^1$ multiplet are foreseen with Z, since the interaction between the three unpaired protons depends on the total number of protons occupying the $\pi g_{7/2}$ orbit. Indeed the two-body interaction evolves from an attractive particle-particle one (for low Z value) to a repulsive particle-hole one (for high Z value). The evolution of the multiplets can be easily predicted following the procedures described in Ref. [24], which have been already used in similar cases [15,25,26]. For that purpose, we only need the values of the residual interactions in the $(\pi g_{7/2})^2$ and $(\pi g_{7/2})^1(\pi d_{5/2})^1$ configurations. They are extracted from the multiplets of states identified in $^{134}_{52}$Te (see Fig. 12).

The results of the computations of the $(\pi g_{7/2})^2(\pi d_{5/2})^1$ configuration are shown in Fig. 13, as compared to the results of the simple configuration, $(\pi g_{7/2})^3$, which is also active in the nuclei of interest. The yrast line of the latter comprises the $7/2^+$, $11/2^+$ and $15/2^+$ states [see Fig. 13(a)]. Noteworthy is the fact that, due to the particle-hole symmetry, the $(\pi g_{7/2})^{-3}$ configuration leads to the same states. On the other hand, three different sets are obtained for the $(\pi g_{7/2})^2(\pi d_{5/2})^1$ configuration, depending on the number of protons filling the $\pi g_{7/2}$ orbit: Fig. 13(b) shows the results obtained for two particles in the $\pi g_{7/2}$ orbit, Fig. 13(c) for mid-occupation of the $\pi g_{7/2}$ orbit (i.e., for 4 particles), and Fig. 13(d) for two holes in the $\pi g_{7/2}$ orbit. It has to be noticed that the yrast lines which extend from $I^\pi = 5/2^+$ to $17/2^+$ do not comprise exactly the same intermediate states. Thus the low-lying yrast states of the odd-Z isotones with $N = 82$ are expected to evolve with Z, as observed in the present work (compare the bottoms of the ^{137}Cs and ^{139}La schemes, Figs. 1 and 3). Moreover this very simple approach may explain why the $17/2^+$ state can suddenly become an isomeric state, as measured in ^{139}La, while no measurable half-life is found in the other odd-Z isotones. Depending on the occupation rate of the $\pi g_{7/2}$ orbit, the $15/2^+$ state belongs to the yrast line or does not belong to it. In the first case, the $M1$ decay of the $17/2^+$ state is fast, while in the second case, the $17/2^+$ state decays by emitting an $E2$ transition of low energy [see, for instance, Fig. 13(c)], which leads to an isomeric state. However we cannot make a one-to-one mapping between the four cases shown in Fig. 13 and the odd-Z isotones, since the two proton orbits are gradually filled together. Thus a shell-model approach with configuration mixings has to be used to precisely discuss the yrast states of the $N = 82$ isotones; this is presented in the next section.

C. Results of shell-model calculations

Many years ago, a first shell-model (SM) analysis was carried out on the proton configurations of the $N = 82$ isotones lying above the doubly-magic ^{132}Sn nucleus [27,28]. The two-body part of the SM Hamiltonian was parametrized in terms of the modified surface delta interaction (MSDI). The parameters of the interaction, as well as the single particle energies, were adjusted in order to give the best fit of the experimental data known at that time. Many years later, using the wealth of new data on the $N = 82$ isotones, Wildenthal has modified a lot of the previously obtained values of the two-body matrix elements (TBMEs) in order to fit as well as possible known excitations energies in nuclei from ^{133}Sb to ^{154}Hf [1]. Then Blomqvist updated these TBMEs using new experimental information in ^{133}Sb – ^{138}Ba: The new set of diagonal and nondiagonal proton-proton matrix elements,

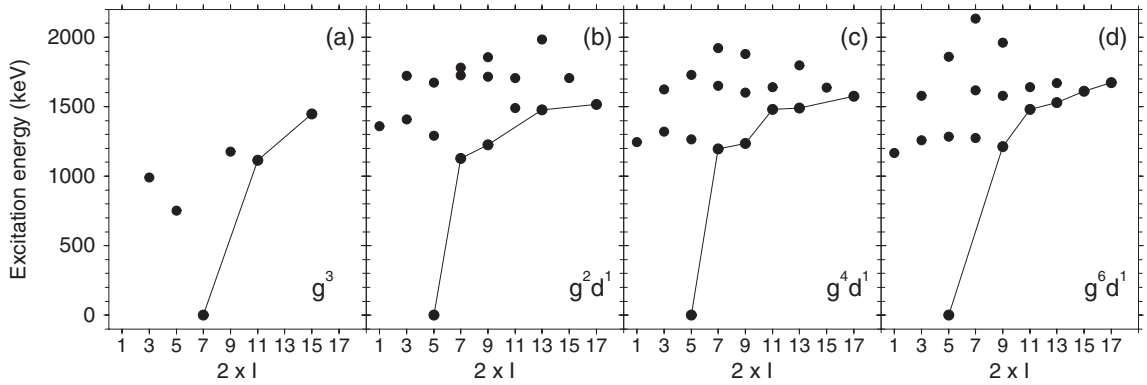

FIG. 13. States issued from four odd-Z configurations, $(\pi g_{7/2})^3$, $(\pi g_{7/2})^2(\pi d_{5/2})^1$, $(\pi g_{7/2})^4(\pi d_{5/2})^1$, and $(\pi g_{7/2})^6(\pi d_{5/2})^1$, calculated using the residual interactions extracted from two multiplets of ^{134}Te (see text). The yrast states are linked by a solid line.

including the five orbits of the 50-82 major shell, is given in Ref. [2]. Afterwards, these empirical effective interactions were used to describe the new yrast level scheme of ^{137}Cs [5]; the calculated energies were found to be very close to the experimental ones.

In this section, we make a detailed comparison between the experimental information obtained in the five $N = 82$ isotones studied in the present work and the SM predictions using these empirical effective interactions [2]. The calculations were performed using the ANTOINE code [29].

1. The even-Z isotones

The results of the SM calculations of the yrast states of ^{136}Xe, ^{138}Ba, and ^{140}Ce are drawn in Fig. 14, where they are compared to the experimental results. The positive-parity states up to the 10^+_1 level in ^{136}Xe and to the 12^+_1 level in ^{138}Ba and ^{140}Ce are obviously well reproduced (see the red asterisks and circles), since they took part of the data set used to fit the two-body matrix elements [2]. For the negative-parity states (drawn in blue), the SM results show that the yrast structures strongly depend on the available configurations. While ^{136}Xe only displays the $14^- \rightarrow 13^- \rightarrow 11^- \rightarrow 9^-$ sequence from the $(\pi g_{7/2}\pi d_{5/2})^3(\pi h_{11/2})^1$ configuration, the addition of the $(\pi g_{7/2}\pi d_{5/2})^5(\pi h_{11/2})^1$ configuration in ^{138}Ba and ^{140}Ce leads to almost regular structures extending up to $I^\pi = 17^-$. This is in good agreement with the new levels observed in ^{138}Ba and ^{140}Ce [see the blue crosses in Figs. 14(b) and 14(c)]. More precisely, two 13^- states are predicted close in energy in ^{138}Ba, as measured experimentally. Their main configurations explain their different decays. The 13^-_1 and 11^-_1 states have the same configuration, $(\pi g_{7/2})^5(\pi h_{11/2})^1$, while the 13^-_2 state has another one, $(\pi g_{7/2})^4(\pi d_{5/2})^1(\pi h_{11/2})^1$. Moreover, the latter configuration is the one of the 14^-_1 state, explaining why this state does not decay to the 13^-_1 state but is only linked to the 13^-_2 state.

As mentioned before (see Table IX), when restricting excitations to the proton valence space, the high values of the angular momenta need to promote a proton pair into the $\pi h_{11/2}$ orbit and to break that pair. In that way and by breaking another pair in the $\pi g_{7/2}$ and $\pi d_{5/2}$ orbits, states with I^π values up to 16^+ are obtained. The multiplet $(12^+ \leqslant I \leqslant 16^+)$ is predicted to be almost degenerated in energy in the three isotones (see the red squares in Fig. 14). In ^{138}Ba and ^{140}Ce, such a structure extends up to higher spin values, as more pairs of protons lying in the $\pi g_{7/2}$ and $\pi d_{5/2}$ orbits can be broken. The resulting levels $(16^+ \leqslant I \leqslant 20^+)$ are no longer degenerated, being spread over an interval of $\sim$2 MeV [see the upper red squares in Figs. 14(b) and 14(c)]. The new structure of ^{136}Xe, which extends from the 5481-keV state to the 7946-keV one [see the red crosses in Fig. 14(a)], is too low in energy to come from the $(\pi g_{7/2})^2(\pi h_{11/2})^2$ configuration. It will be discussed in Sec. IV D in terms of neutron excitation across the $N = 82$ gap, as was already done for the highest-spin states observed in ^{134}Te [3]. The behavior of ^{138}Ba is more complex. The SM results fit reasonably well the high part of the experimental sequence [from the (14^+_2) state to the (20^+) one] but not its low part [from the (11^+) state to the (14^+_1) one]. Thus the latter is likely issued from the neutron excitation across the $N = 82$ gap, while the configuration of the former is likely $(\pi g_{7/2}\pi d_{5/2})^4(\pi h_{11/2})^2$.

For ^{140}Ce, because of its low population in the reactions used in the present work, no cascade of low-energy transitions lying in the top of its level scheme could be observed, thus its highest-spin states with positive parity remain unobserved.

2. The odd-Z isotones

When Blomqvist updated the TBME values [2], the states of ^{137}Cs having $I^\pi \geqslant 11/2$ were not yet identified, thus they were not considered in the fit. Some time later, the newly observed levels of ^{137}Cs were compared to the theoretical results, showing a very good agreement [5]. Results of the calculations of the yrast states, as well as some of them close to the yrast line, are shown in Fig. 15 (see the circles), in comparison with the experimental results (drawn with asterisks and crosses). The theoretical yrast line displays several irregularities. For instance, the two $19/2^+$ states are located above the first $21/2^+$ state, thus the latter decays directly toward the $17/2^+$ state. As well, the $13/2^+_1$ state is located higher in energy than the $15/2^+_1$ one, thus the latter decays toward the $11/2^+$ state.

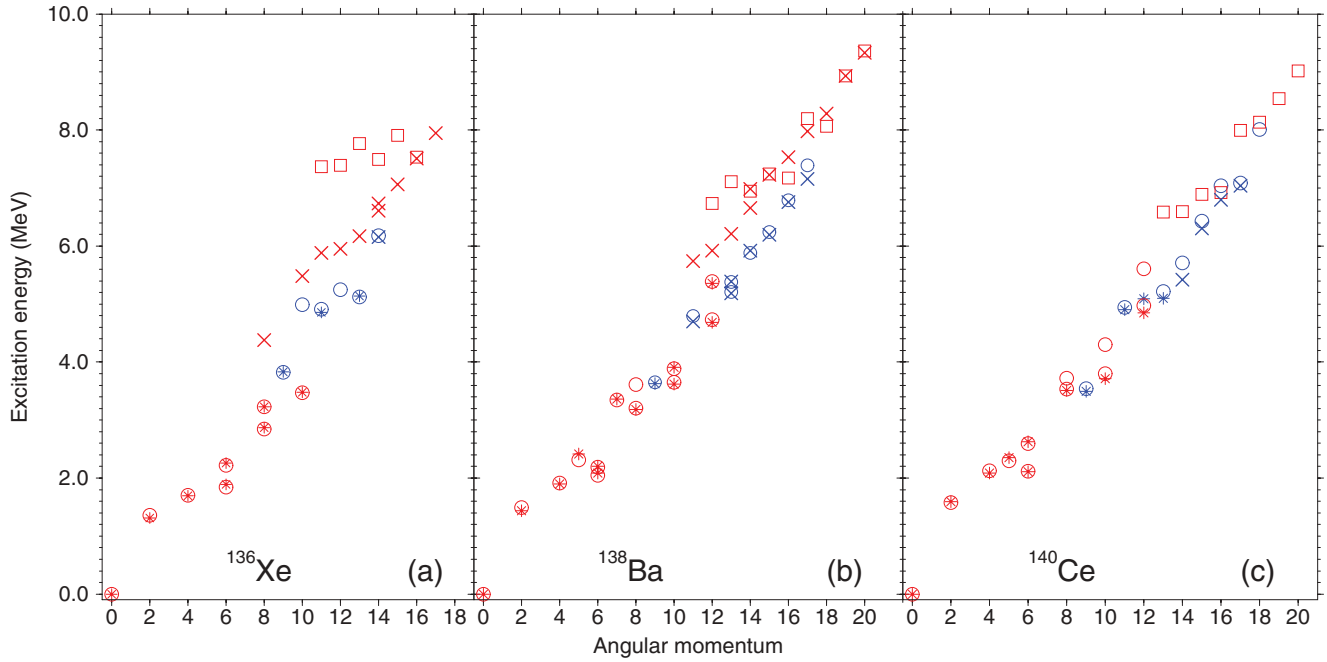

FIG. 14. (Color online) Excitation energy as a function of angular momentum of the states of ^{136}Xe (a), ^{138}Ba (b), and ^{140}Ce (c). The positive-parity states predicted by the SM calculations are drawn with red circles when issued from the $(\pi g_{7/2}\pi d_{5/2})^n$ configurations and with red squares when issued from the $(\pi g_{7/2}\pi d_{5/2})^{n-2}(\pi h_{11/2})^2$ configurations. The negative-parity states predicted by the SM calculations are drawn with blue circles. The new experimental states identified in this work are drawn with crosses. The experimental states, which were used to fit the two-body matrix elements (see text), are drawn with asterisks. The red (blue) color is used for positive (negative) parity states.

The negative-parity states behave similarly. The $25/2_1^-$ state is located higher in energy than the $27/2_1^-$ one, thus the latter decays toward the $23/2^-$ state, as observed experimentally. The predicted behavior of the first states is very peculiar, showing a quasi-degeneracy of the six states with $I^\pi = 13/2^- - 23/2^-$. This explains why the three observed states ($19/2^-$, $21/2^-$, and $23/2^-$) only decay to the positive-parity states.

As discussed in Sec. IV A, a proton pair has to be promoted to the $\pi h_{11/2}$ orbit in order to describe the higher values of angular momentum (see the bottom part of Table IX). The calculated states of ^{137}Cs having the $(\pi g_{7/2}\pi d_{5/2})^3(\pi h_{11/2})^2$ configuration are shown in Fig. 16 (see the circles). The yrast line is irregular, several states being predicted to be very close in energy. Nevertheless, this line is not far from

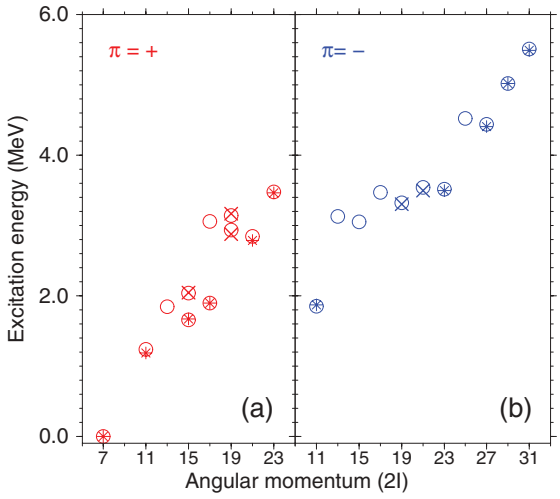

FIG. 15. (Color online) Excitation energy as a function of angular momentum of the states of ^{137}Cs. The states predicted by the SM calculations for the $(\pi g_{7/2}\pi d_{5/2})^5$ (a) and $(\pi g_{7/2}\pi d_{5/2})^4(\pi h_{11/2})^1$ configuration (b) are drawn with circles. The new experimental states identified in this work are drawn with crosses. The already known experimental states are drawn with asterisks, a few of them were used to fit the two-body matrix elements (see text).

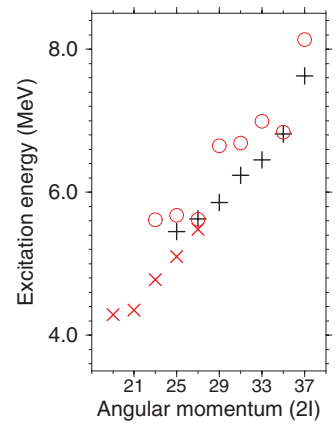

FIG. 16. (Color online) High-energy level scheme of ^{137}Cs. States of structure C are drawn with × and those of structure D with +. The SM states from the $(\pi g_{7/2}\pi d_{5/2})^3(\pi h_{11/2})^2$ configuration are drawn with circles.

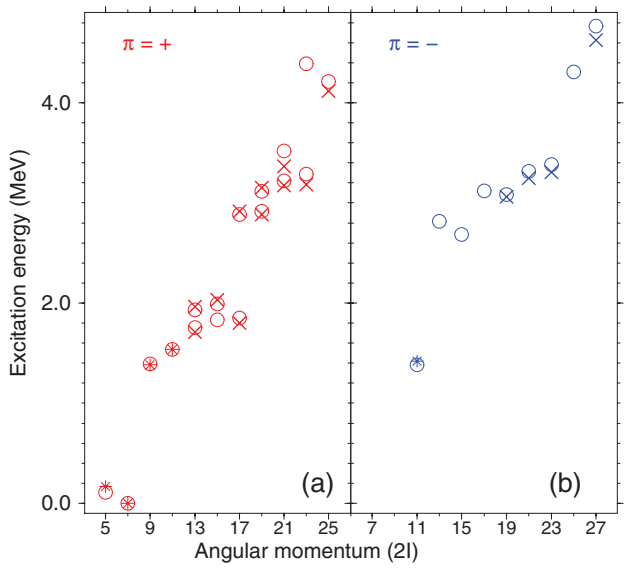

FIG. 17. (Color online) Excitation energy as a function of angular momentum of the states of ^{139}La. The states predicted by the SM calculations are drawn with circles. The new experimental states identified in this work are drawn with crosses. The experimental states, which were used to fit the two-body matrix elements (see text), are drawn with asterisks.

TABLE X. Comparison of experimental and calculated energies of the yrast states of ^{139}La. The TBME values used in the SM calculations are those of Ref. [2].

I^π	$E_{\rm exp}$ (keV)	$E_{\rm SM}$ (keV)	$E_{\rm exp} - E_{\rm SM}$ (keV)
$7/2^+$	0	0	0
$5/2^+$	166	109	+57
$9/2^+$	1381	1394	−13
$11/2^-$	1420	1382	+38
$11/2^+$	1537	1538	−1
$13/2_1^+$	1711	1756	−45
$15/2_1^+$		1832	
$17/2^+$	1800	1852	−52
$13/2_2^+$	1962	1933	+29
$15/2_2^+$	2032	1991	+41
$19/2_1^+$	2885	2915	−30
$17/2^+$	2917	2882	+35
$19/2^-$	3060	3085	−25
$19/2_2^+$	3150	3115	+35
$21/2_1^+$	3175	3218	−43
$23/2^+$	3184	3287	−103
$23/2^-$	3305	3384	−79
$21/2_2^+$	3364	3518	−154
$25/2^+$	4116	4214	−98
$27/2^-$	4627	4765	−138

the states of Structure D (see the + symbols in Fig. 16). Thus the main configuration of the states of Structure D is likely $(\pi g_{7/2}\pi d_{5/2})^3(\pi h_{11/2})^2$. On the other hand, states of Structure C are too low in energy to be explained in terms of proton excitations (see the × symbols in Fig. 16). As already discussed in Sec. IV C1 for ^{136}Xe and ^{138}Ba, neutron excitation across the $N = 82$ gap has to be considered (cf. the next section, Sec. IV D).

Results of calculations performed for ^{139}La are shown in Fig. 17 (see the circles), where we have drawn one or two states for each spin value. First of all, it is important to notice that the positive-parity yrast line is different from the results obtained in ^{137}Cs. Indeed several states of ^{139}La are found at lower energy and can now take part in the yrast decay, such as the $9/2_1^+$, $13/2_1^+$, and $19/2_1^+$ states. This change is related to the discussion in Sec. IV B. It is worth noting that the $15/2_1^+$ state is predicted to lie 20 keV below the $17/2_1^+$ state, thus the latter would not exhibit any delayed decay. This is at variance with the experimental results showing an isomeric state with $T_{1/2} = 315$ ns. We surmise that the energy of the $15/2_1^+$ state is predicted slightly too low. Such a discrepancy is in agreement with the observed deviations between the experimental and calculated energies; see for instance Table III of Ref. [2] for the light-A isotones and Table X (this work) for ^{139}La.

All the experimental states observed below 4116 keV have a theoretical counterpart (see the stars and the crosses in Fig. 17). For the $15/2^+$ states, only one experimental level is proposed at 2032 keV, which is close to the prediction of the $15/2_2^+$ state. The fact that the $15/2_1^+$ state was not populated in our experiment could be explained by its configuration,$(\pi g_{7/2})^6(\pi d_{5/2})^1$, which is different from the one of the states lying above it; the $17/2_2^+$, $19/2_1^+$, and $19/2_2^+$ states have the same configuration, $(\pi g_{7/2})^5(\pi d_{5/2})^2$. It is important to note that the experimental $21/2_2^+$, $23/2^+$ and $25/2^+$ states are located at lower energies than the calculated ones, the deviations being ∼100 keV (Table X). This could be related to interactions between the states due to proton excitations among the $\pi g_{7/2}$ and $\pi d_{5/2}$ orbits (belonging to the valence space used in the SM calculations) and the states of Structure C (see Fig. 3).

Finally, the states of Structure C would be likely due to the breaking of the neutron core, as the corresponding states of ^{137}Cs. Nevertheless, since the high-spin states having a broken proton pair in the $\pi h_{11/2}$ orbit are predicted to be at lower energy than in ^{137}Cs (about 600 keV less), we expect large mixings of these two excitation modes in ^{139}La.

3. Conclusion

This set of empirical effective interactions within the proton valence space including all the orbits of the 50-82 major shell describes well the yrast states of the five isotones studied in the present work, both the even-Z and the odd-Z ones. The deviations between experimental and calculated energies are mostly below 50 keV, which is much better than the values obtained for SM calculations using effective interactions derived from the nucleon-nucleon potential, such as was done for one prediction of the yrast states of ^{137}Cs (see Table II of Ref. [17]). The latter approach is broader since it can be used in all the valence spaces, thus it would be interesting to compare the numerical values of the two sets in order to find whether some particular TBMEs are at the origin of

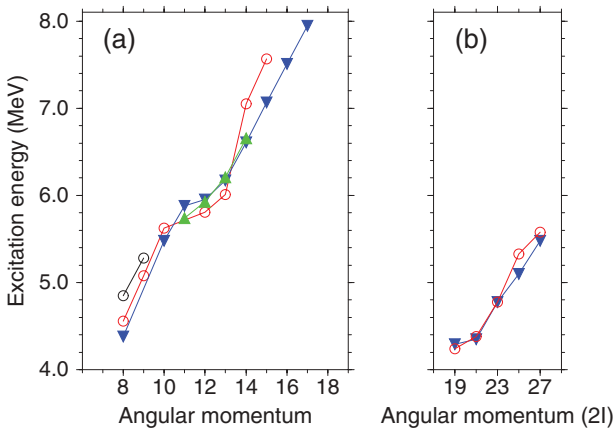

FIG. 18. (Color online) Excitation energy as a function of angular momentum of the states proposed to be due to neutron excitation across the $N = 82$ gap, i.e. having the main configuration, $(\pi g_{7/2}\pi d_{5/2})^n \otimes (\nu h_{11/2})^{-1}(\nu f_{7/2})^{+1}$. (a) $n = 0$ for ^{132}Sn (black circles), $n = 2$ for ^{134}Te (red circles), $n = 4$ for ^{136}Xe (blue triangles), and $n = 6$ for ^{138}Ba (green triangles). (b) $n = 3$ for ^{135}I (red circles) and $n = 5$ for ^{137}Cs (blue triangles) (data from Ref. [18] and this work).

the better description and to understand why they would be unsatisfactorily calculated from the nucleon-nucleon potential.

D. Neutron-core excitation

The neutron excitation of the doubly-magic ^{132}Sn nucleus gives rise to its first positive-parity excited states: The multiplet from the $(\nu h_{11/2})^{-1}(\nu f_{7/2})^{+1}$ configuration was measured in the 4–5 MeV energy range, with spin values extending from 2^+ to 9^+ [30,31]. In ^{134}Te, states with higher spin values are obtained, as this first neutron-core excitation can be coupled to the breaking of the proton pair [3] [see the red circles in Fig. 18(a)]. The states of ^{136}Xe, drawn with crosses in Fig. 14(a), extend from 4379 keV [$I^\pi = (8^+)$] to 7946 keV [$I^\pi = (17^+)$]. They fit well with those due to the neutron-core breaking of ^{134}Te [compare the blue triangles and the red circles in Fig. 18(a)]. Finally, the states of ^{138}Ba extending from 5740 keV [$I^\pi = (11^+)$] to 6656 keV [$I^\pi = (14^+)$] are in good agreement with those of the lighter isotones [see the green triangles in Fig. 18(a)]. The closeness of the states of ^{134}Te, ^{136}Xe, and ^{138}Ba involving the neutron-core excitation is due to the stability of the gap in energy between the $\nu h_{11/2}$ and the $\nu f_{7/2}$ orbits, as shown in Fig. 38 of Ref. [32].

For the breaking of the neutron core in the odd-Z isotones, we compare in Fig. 18(b) the states of ^{135}I lying between 4241 and 5576 keV [3] and those of Structure C of ^{137}Cs, neither of them described by SM calculations within the proton space (see Ref. [3] and Sec. IV C2). They show the same behavior and are in good agreement with the corresponding states of the even-Z isotones.

Even though the configurations of the highest-spin states of ^{137}Cs and ^{138}Ba observed in the present work can be $(\pi g_{7/2}\pi d_{5/2})^3(\pi h_{11/2})^2$ and $(\pi g_{7/2}\pi d_{5/2})^4(\pi h_{11/2})^2$, respectively (see Secs. IV C2 and IV C1), we cannot exclude other configurations involving the breaking of the neutron core, such as $(\pi g_{7/2}\pi d_{5/2})^5(\nu h_{11/2})^{-1}(\nu f_{7/2})^{+1}$ and $(\pi g_{7/2}\pi d_{5/2})^6(\nu h_{11/2})^{-1}(\nu f_{7/2})^{+1}$, respectively.

V. SUMMARY

Five $N = 82$ isotones have been produced as fission fragments in two fusion reactions, ^{12}C + ^{238}U at 90 MeV and ^{18}O + ^{208}Pb at 85 MeV. Their high-spin level schemes have been built by analyzing the triple γ-ray coincidence data obtained with the Euroball array. In order to identify the new transitions of ^{139}La, we have used their coincidences with the lines emitted by its complementary fragments. Moreover, the use of the fission-fragment detector, SAPhIR, has allowed us to identify a new isomeric state in ^{139}La, at 1800 keV excitation energy. Spin and parity values of several excited states of ^{136}Xe and ^{137}Cs could be assigned from the results of γ-γ angular correlations. All the states observed in these $N = 82$ isotones have been compared to results of shell model calculations performed in the 50-82 proton valence space and using empirical effective interactions which had been fitted on previous experimental data. Most of the yrast states of the five $N = 82$ isotones are very well described by this approach. In addition, the excitation of the $N = 82$ core gives rise to several structures which have been clearly identified in ^{136}Xe, ^{137}Cs, and ^{138}Ba.

ACKNOWLEDGMENTS

The Euroball project was a collaboration among France, the United Kingdom, Germany, Italy, Denmark and Sweden. The first experiment was performed under U.E. Contract No. ERB FHGECT 980 110 at Legnaro. The second experiment was supported in part by the EU under Contract No. HPRI-CT-1999-00078 (EUROVIV). We thank many colleagues for their active participation in the experiments: A. Bogachev, A. Buta, J. L. Durell, Th. Ethvignot, F. Khalfalla, I. Piqueras, A. A. Roach, A. G. Smith, and B. J. Varley. We thank the crews of the Vivitron. We are very indebted to M.-A. Saettle for preparing the Pb target, and to P. Bednarczyk, J. Devin, J.-M. Gallone, P. Médina, and D. Vintache for their help during the experiment.

[1] B. H. Wildenthal, in *Understanding the Variety of Nuclear Excitations: Proceedings of the 3rd International Spring Seminar on Nuclear Physics, Ischia, 1990*, edited by A. Covello (World Scientific, Singapore, 1991), p. 35.
[2] J. Blomqvist, Acta Phys. Pol. B **30**, 697 (1999).
[3] C. T. Zhang *et al.*, Phys. Rev. Lett. **77**, 3743 (1996).
[4] P. J. Daly *et al.*, Phys. Rev. C **59**, 3066 (1999).
[5] R. Broda *et al.*, Phys. Rev. C **59**, 3071 (1999).
[6] J. Simpson, Z. Phys. A **358**, 139 (1997); F. A. Beck, Prog. Part. Nucl. Phys. A **28**, 443 (1992).
[7] J. Eberth *et al.*, Nucl. Instrum. Methods, Sect. A **369**, 135 (1996).

[8] G. Duchêne *et al.*, Nucl. Instrum. Methods, Sect. A **432**, 90 (1999).
[9] D. Radford, Nucl. Instrum. Methods, Sect. A **361**, 297 (1995).
[10] M. A. C. Hotchkis *et al.*, Nucl. Phys. A **530**, 111 (1991).
[11] M.-G. Porquet *et al.*, Acta Phys. Pol. B **27**, 179 (1996).
[12] R. Lucas *et al.*, Eur. Phys. J. A **15**, 315 (2002).
[13] M.-G. Porquet *et al.*, Eur. Phys. J. A **24**, 39 (2005).
[14] Ch. Theisen *et al.*, in *Proceedings of the 2nd International Workshop on Nuclear Fission and Fission Product Spectroscopy, Seyssins, France, April 1998*, AIP Conf. Proc. No. 447 (AIP, New York, 1998), p. 143.
[15] A. Astier *et al.*, Eur. Phys. J. A **30**, 541 (2006).
[16] M.-G. Porquet *et al.*, Phys. Rev. C **84**, 054305 (2011).
[17] K. Li *et al.*, Phys. Rev. C **75**, 044314 (2007).
[18] ENSDF database, [http://www.nndc.bnl.gov/ensdf/].
[19] J. K. Hwang *et al.*, Phys. Rev. C **58**, 3252 (1998).
[20] H. Prade, W. Enghardt, H. U. Jäger, L. Käubler, H.-J. Keller, and F. Stary, Nucl. Phys. A **370**, 47 (1981).
[21] H. Prade *et al.*, Nucl. Phys. A **472**, 381 (1987).
[22] P. H. Regan *et al.*, Acta Phys. Pol. B **36**, 1313 (2005).
[23] W. Enghardt, H. U. Jäger, L. Käubler, H.-J. Keller, H. Prade, and F. Stary, Nucl. Phys. A **449**, 417 (1986).
[24] I. Talmi, *Simple Models of Complex Nuclei* (Harwood Academic, Chur, Switzerland, 1993).
[25] A. Astier and M.-G. Porquet, Phys. Rev. C **83**, 034302 (2011).
[26] M.-G. Porquet *et al.*, Eur. Phys. J. A **20**, 245 (2004).
[27] B. H. Wildenthal, Phys. Rev. Lett. **22**, 1118 (1969).
[28] B. H. Wildenthal and D. Larson, Phys. Lett. b **37**, 266 (1971).
[29] E. Caurier and F. Nowacki, Acta Phys. Pol. B **30**, 705 (1999).
[30] B. Fogelberg *et al.*, Phys. Scripta T **56**, 79 (1995).
[31] P. Bhattacharyya *et al.*, Phys. Rev. Lett. **87**, 062502 (2001).
[32] O. Sorlin and M.-G. Porquet, Prog. Part. Nucl. Phys. **61**, 602 (2008).